# CALIFORNIA INSTITUTE OF TECHNOLOGY

EARTHQUAKE ENGINEERING RESEARCH LABORATORY

# HIGH FREQUENCY ERRORS AND INSTRUMENT CORRECTIONS OF STRONG-MOTION ACCELEROGRAMS

BY

M. D. TRIFUNAC, F. E. UDWADIA AND A. G. BRADY

EERL 71-05

PASADENA, CALIFORNIA

JULY, 1971

CALIFORNIA INSTITUTE OF TECHNOLOGY

EARTHQUAKE ENGINEERING RESEARCH LABORATORY

# HIGH FREQUENCY ERRORS AND INSTRUMENT
# CORRECTIONS OF STRONG-MOTION ACCELEROGRAMS

By

M. D. Trifunac, F. E. Udwadia and A. G. Brady

# ABSTRACT

A study of high-frequency errors present in digitized accelero-grams and an analysis of the distribution of unequally spaced, hand-digitized data indicates that the Fourier content of digitized accelerogram data may be accurate up to about 25 cps.

Two methods for accelerometer instrument correction are described: (1) a direct numerical differentiation of recorded accelerograms from which high-frequency digitization errors have been filtered out and (2) an ideal "mathematical accelerometer" with a natural frequency significantly higher than the natural frequency of the recording instrument. Although both methods give good results, the first one is recommended for the standard use.

## INTRODUCTION

Information on a detailed time history of strong ground motion comes from accelerographs. These instruments usually record one vertical and two horizontal components of ground acceleration (Trifunac and Hudson 1970). Accelerograph records are then used by earthquake engineers to study the design of earthquake-resistant structures and by strong-motion seismologists to study the basic properties of the earthquake source mechanism. Since recorded ground acceleration represents the main source of basic experimental measurements, it is essential to retrieve the maximum available information contained in these records.

To record ground acceleration, the relative response of a single degree of freedom oscillator viscously damped is usually employed. The natural frequency of such a transducer is between 10 and 30 cps, while the equivalent viscous damping is about 60 percent of critical. The recorded relative instrument response approximates accurately the ground acceleration in the frequency range from 0 cps to about 1/2 to 3/4 of the natural frequency of the transducer. Thus, the direct instrument output can be used to represent ground acceleration up to about 5 to 15 cps. If information on higher frequencies is required, instrument correction of the recorded accelerogram must be performed.

Modern computational methods in the dynamics of structures now also require the accurate high-frequency part of the accelerogram, in order to determine the response of the higher modes of vibration. Detailed studies of earthquake source parameters and especially the studies aimed at the determination of the size of the earthquake dislocation surface and the effective stress, call for the maximum possible accuracy in the high-frequency end of the Fourier amplitude spectrum

of ground acceleration.

There are two basic steps in the processing of recorded strong-motion accelerograms. One is the baseline correction (Trifunac 1970) and the other, considered in this paper, is the instrument correction. To determine optimum instrument-correction procedures, it becomes necessary to analyze various high-frequency errors that are present in uncorrected, hand-digitized paper-accelerograms. This analysis is presented in the first part of this paper.

Unlike the baseline correction of accelerograms (Trifunac 1970) considered by many investigators, the instrument correction problem was studied by only a few. Jenschke and Penzien (1964) proposed an approximate method for the accelerograph instrument correction in response spectrum calculations. Their method was based on a numerical approximation of the first derivative of an accelerograph transducer's recorded relative response, whereas McLennan (1969) derived an exact method to correct for accelerometer error in the dynamic response calculations. The disadvantage in both of these methods was that they were designed to correct the response spectra and not the recorded accelerogram that serves as the basic input for all computations.

In the second part of this paper we present two different types of accelerometer instrument corrections. The first method, based on our previous work (Trifunac and Hudson 1970), is exact and uses direct numerical differentiation of an instrument response. This differentiation is performed after high frequency digitization errors are filtered out from digitized data. The second method is the extension of McLennan's (1969) approach. It consists of computing the response of a high-frequency oscillator that has a natural frequency significantly higher than the accelerometer frequency.

## ANALYSIS OF HIGH-FREQUENCY ERRORS

### High-Frequency Errors in Digitized Accelerograms

To determine the high-frequency domain in which uncorrected, digitized, accelerogram data may be used and to generate corrected accelerograms, a study has been made of errors present in the raw digitized data. These errors come from various sources and are in many cases represented by the properties of each instrument. Since this study is mainly motivated by a need for a uniform, standard processing of existing strong-motion accelerograms on paper and film, we will consider mainly those errors common to all records and will disregard some minor changes caused by differences in instrument design.

Most high-frequency errors can be divided into several groups:

1. Modifications of the harmonic amplitudes and phase shifts caused by the finite natural frequency $\omega_o$ of the acceleration transducer.

2. The errors resulting from imperfections in the transducer design.

3. Random digitization errors.

4. The errors caused by inadequate resolution of digitizing equipment.

5. Low-pass filtering effects in the mechanical-optical digitization process.

There are also other types of errors present in analog accelerogram traces. Examples are errors caused by the transverse play of recording paper or film in the drive mechanism, warping of records from photographic processing and aging, use of 70 mm and 35 mm film negatives and the imperfect mechanical traverse mechanism of the

cross-hair system on the digitizing table (Trifunac, 1970). Although all these errors may contain some high-frequency components in the frequency range investigated here, past experience with typical accelerograms recorded mainly on light-sensitive paper indicates that these errors are negligible compared to the five main sources of errors listed above. We shall now consider each of these errors and describe how they affect the accuracy of the digitized accelerograms in the high-frequency domain.

1. Transducer distortions of amplitude and phase. Modifications of harmonic amplitudes and phases of original input signals may be caused by the relatively low natural frequency of a transducer element. Most mechanical-optical strong-motion accelerographs commonly deployed have transducers with natural frequencies between 10 cps and 30 cps and about 60 to 70 percent of critical damping. The relative motion x of the transducer mass is given by the differential equation:

$$\ddot{x} + 2\omega_o \zeta_o \dot{x} + \omega_o^2 x = -a$$

where $\zeta_o$ is a fraction of critical damping, $\omega_o$ is the natural frequency ($\omega_o = 2\pi f_o$) and a is the absolute ground acceleration. For the acceleration transducers the largest possible $\omega_o$ is chosen so that the term $\omega_o^2 x$ dominates on the left-hand side of the equation. For input frequencies $\omega$ that are several times smaller than $\omega_o$, $\ddot{x}$ and $2\omega_o \zeta_o \dot{x}$ are small, and $\omega_o^2 x$ is nearly the same as -a (Figure 1a, b). For the higher input frequencies both amplitudes and phases are modified and the correction terms involving $\ddot{x}$ and $2\omega_o \zeta_o \dot{x}$ may not be neglected.

2. Imperfections in the transducer design. To simplify instrument response interpretation, the strong-motion acceleration transducers should be designed to represent a single-degree-of-freedom oscillator viscously damped. Unfortunately it is not always feasible to design an ideal single-degree-of-freedom oscillator, so that most of the transducers
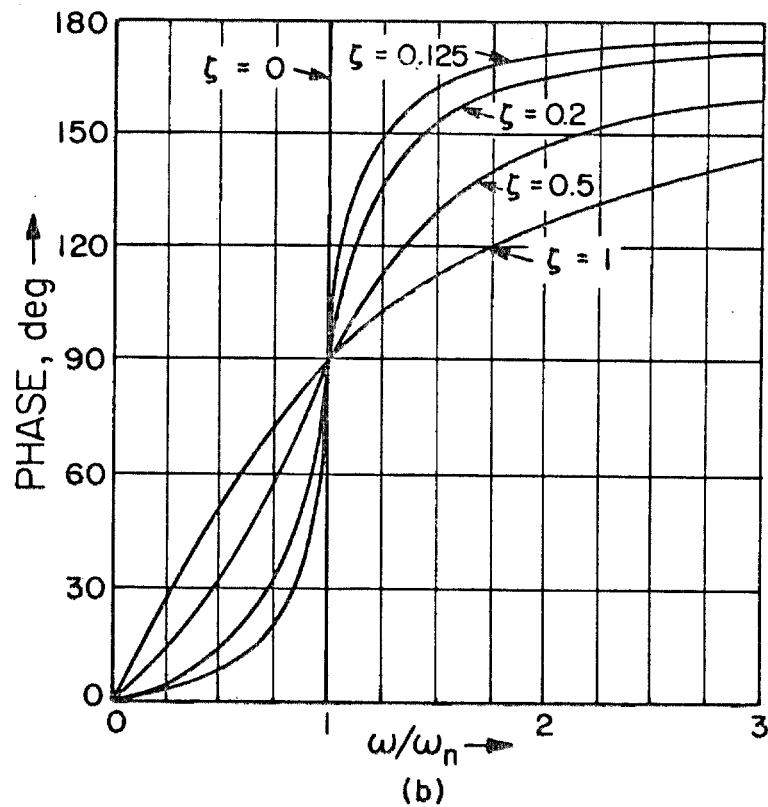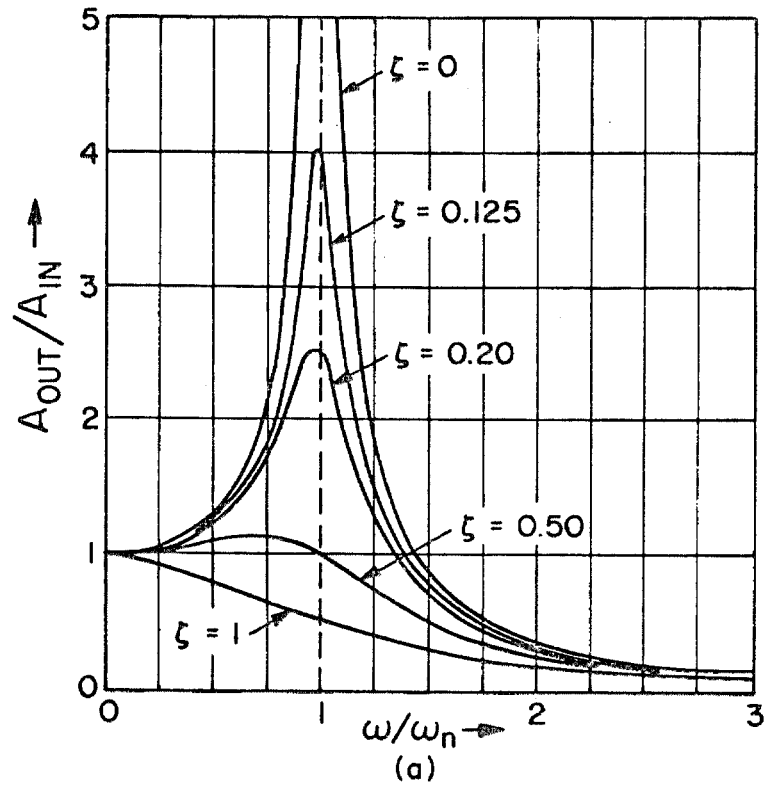
THE SINGLE-DEGREE-OF-FREEDOM SYSTEM



Figure 1

presently existing are essentially multi-degree-of-freedom systems. Their design is aimed at using only the fundamental mode of vibration so that the higher modes will not be excited to the extent that the simplified theory based on a single-degree-of-freedom oscillator cannot be applied. Since most accelerometers are used for frequencies lower than the fundamental frequency of the transducer, these simplifying assumptions are quite justified in most cases.

To demonstrate modes other than fundamental, we might consider the transducer shown in Figure 2, which gives a schematic represent-ation of the element used in the Kinemetrics SMA-1 instrument. Supported by two leaf springs the transducer mass is meant to vibrate in its funda-mental transverse mode only. However, in addition to the higher modes in the transverse direction, the transducer configuration allows tor-sional vibrations as well. These torsional vibrations may be excited by the slight eccentricity of the elctromagnetic damping force. A natural frequency of almost 30 cps was observed during the overall evaluation and testing of the SMA-1 transducer (Trifunac and Hudson 1970), which might be associated with this torsional mode. Although not sig-nificant for ordinary recording of low-frequency signals, such higher modes might affect instrument correction procedures that are based on the simplified single-degree-of-freedom theory. A similar phenomenon is observed in other standard accelerographs such as U.S.C.S.C., AR-240 and RFT-280 which use torsional type transducer systems. In this type of suspension a higher lateral mode the so called "bow string" mode is occa-sionally observed on records, usually caused by some shock excitation.

Other transducer systems have other imperfections. The import-ance of these imperfections may be roughly judged from the point of view of instrument correction, by the closeness of the extraneous
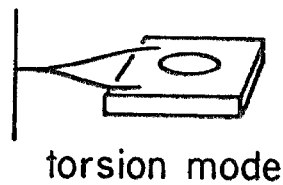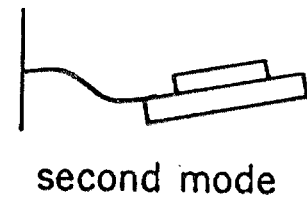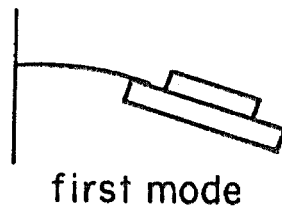
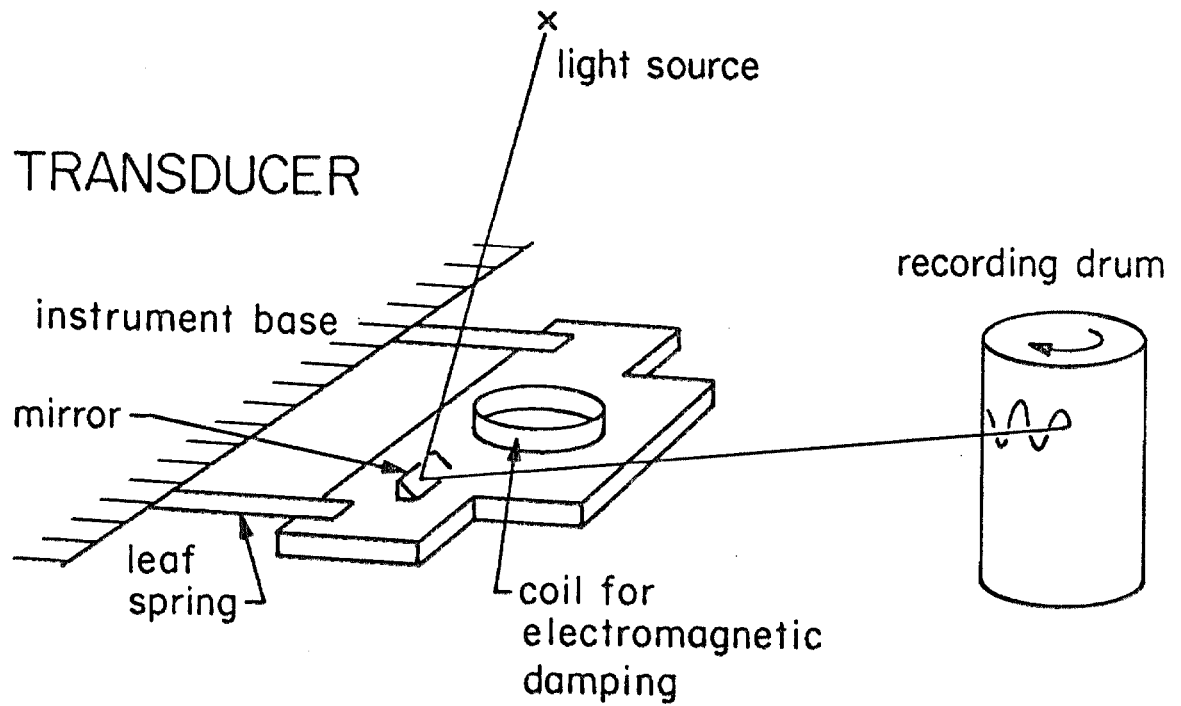# SCHEMATIC REPRESENTATION OF TRANSDUCER



Figure 2. An illustration of the second translational mode and the torsional mode of vibration of a typical transducer.

frequency to the fundamental frequency. For most instruments used to record ground acceleration, these transducer imperfections are relatively small in the 0 to about 25 cps range.

3. Random digitization errors. The process of optical digitization introduces errors which are of three basic kinds:

a) "human error", because of the inability of the operator to pick out the centerline of the analog trace,

b) "discretization error", because the accuracy of the digital data is limited to one digitizer unit, and

c) "systematic error" built into the optical digitizing system.

The first two shall be collectively referred to as random digitization errors.

Figure 3 shows part of a typical photographically recorded trace. During the digitization process the operator attempts to align the cross hair with the center of a trace (indicated by a dashed line in Figure 3). Our recent study (Trifunac, 1970) demonstrated that if the operator is careful, is not biased in choosing the points, and the digitization of every point is independent of the previous ones the errors are nearly normally distributed with zero mean and the average standard deviation $\sigma \approx 1/300$ cm. This standard deviation (Trifunac, 1970) may be affected by the equipment used for this particular study (Benson Lehner 099D Datareducer) but is probably a good estimate of many sets of random digitization errors on other equipment as well. These errors are the main reason why one cannot differentiate the digitized data without a serious high-frequency noise problem.

In a recent preliminary study, Trifunac and Hudson (1970) showed that simple smoothing procedures may be used to filter out most of the

ENLARGED PORTION OF A TYPICAL
OPTICALLY RECORDED ACCELEROGRAPH RECORD
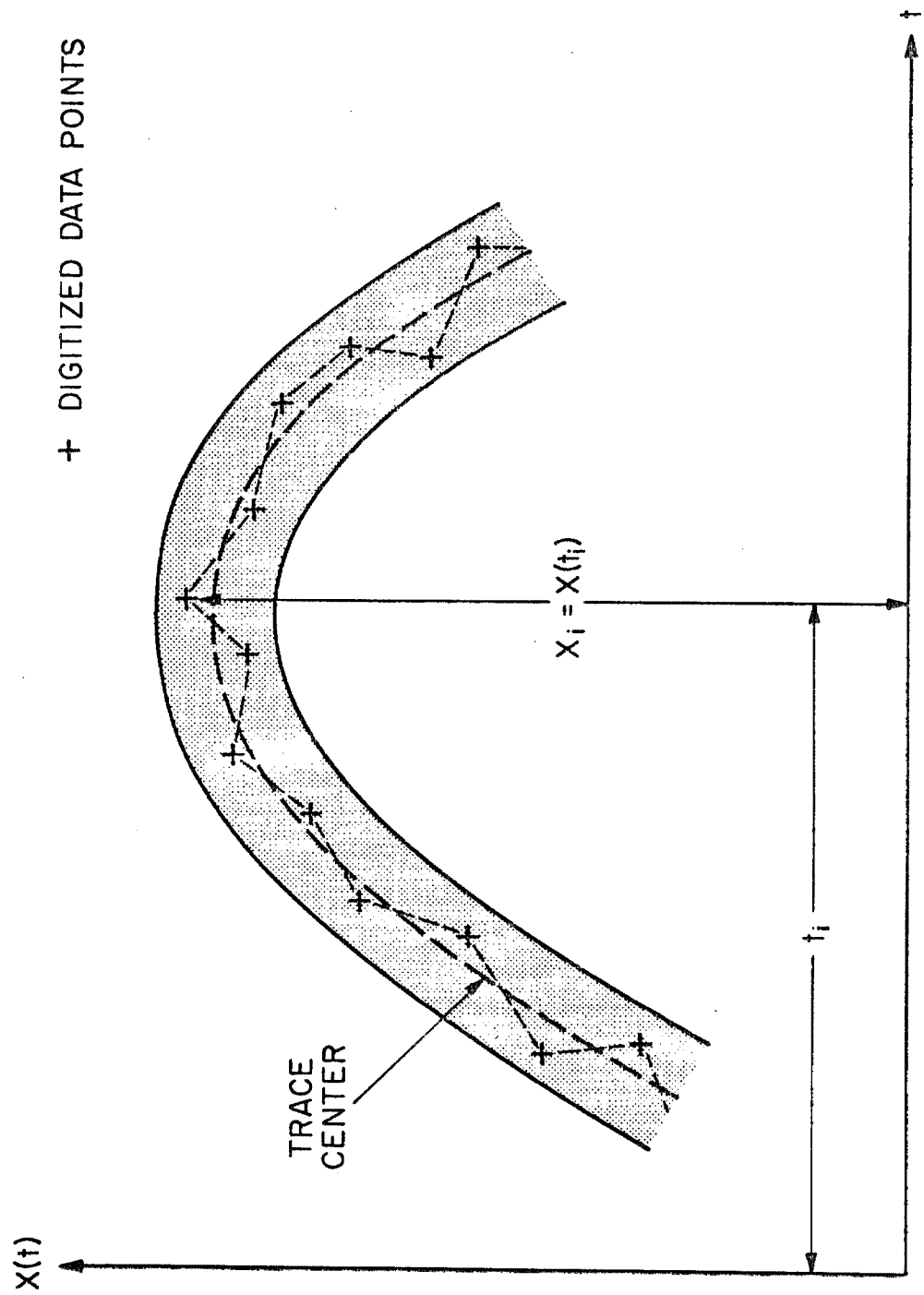
+ DIGITIZED DATA POINTS

Figure 3

high-frequency digitization noise. To advance this method, we
analyze here, in greater detail, the properties of high-frequency
errors in a digitized accelerogram.

Trifunac (1970) performed an experiment which we shall briefly
outline here. A sloping straight line was digitized five times by four
operators. One operator repeated the digitization and used a magni-
fying glass to see whether there was a significant improvement in the
accuracy of the digitization. Since it was taken under essentially
the same conditions as the other four, and there was only a slight
improvement, that digitization was taken as another independent
trial. After five digitizations were completed, the sloping straight
line was least-square fitted to each set of data, translating and rotating
it to a horizontal. The five sets of data obtained in this way are shown
in Figure 4. In order to maintain the generality of these results, the
straight lines (Figure 4), here treated as accelerograms, are given
in units of $pts/cm^2$, where one point corresponds to a unit of the
vertical digitized scale equal to $1/312$ cm and the horizontal axis is
measured in cm.

Since the digitizing errors are nearly normally distributed, with
zero mean, across the ensemble of five sequences, by averaging the five
digitizations one can approximately eliminate random errors and
by subtraction obtain systematic errors caused by imperfect digit-
izing equipment (Trifunac, 1970). The average of the digitizations is
also shown in Figure 4. Differences between each individual digitiza-
tion $Z_i$ and the average $\overline{Z}$ then approximately represent the random
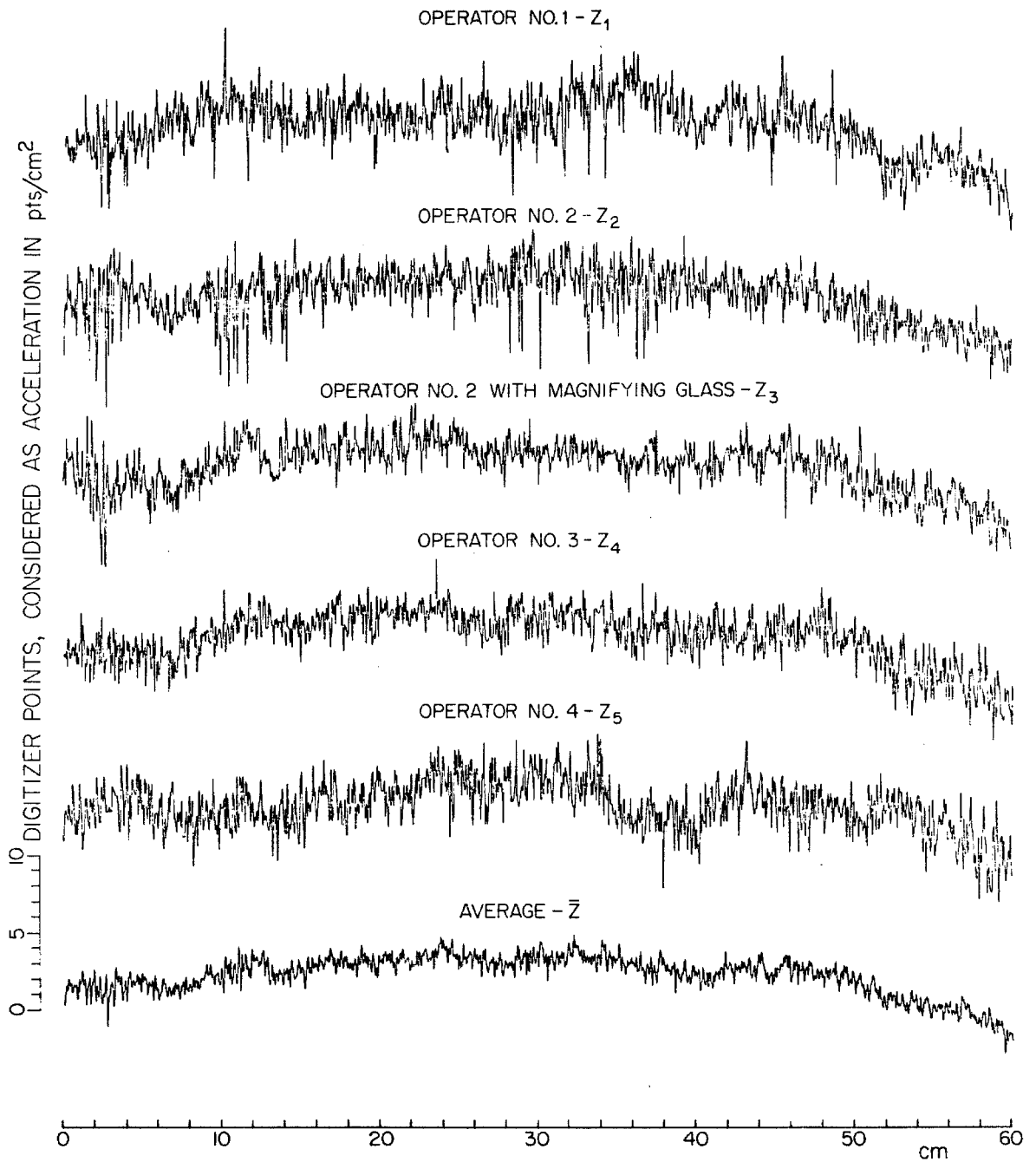digitization errors.

STRAIGHT LINE DIGITIZATION



Figure 4

Predominant frequencies in random digitization errors were obtained by averaging the five Fourier amplitude spectra computed for each $Z_i - \bar{Z}$ . The average of the five spectra is given in Figure 5.

For instrument correction it is necessary to differentiate the digitized function twice. As already mentioned, such a process amplifies high-frequency random digitization errors. To show the Fourier amplitude spectrum of these errors, five Fourier spectra calculated for five differences $Z_i - \bar{Z}$ were multiplied by $\omega^2$ and averaged. The result is shown in Figure 6.

The resolution of a human eye is limited by the wavelength of visible light (about $5 \times 10^{-4}$ mm). The actual resolution during the digitization process is further significantly reduced because of the thickness of the digitizer cross-hair and the parallax. The parallax on the 099D Benson Lehner datareducer amounts to one to two digitizer points (1 point = 1/312 cm) and is treated here as part of the random digitization errors.

The relative importance of the two main constituents of the random digitization error, namely the human error and the discretizing error can be studied in further detail as far as their effect on the final probability distribution of the total error is concerned.

(a) <u>Human error</u>: Denoting the human error in choosing the center-line of the trace by $\epsilon$ , its probability distribution can be approximated by one of those shown in Figure 7a and b.

When the trace is thin, the distribution would be relatively constant across the thickness of the line. As the thickness of the line increases, the distribution will have a larger spread but will be more peaked towards the center. From the above distribution it may then be noted
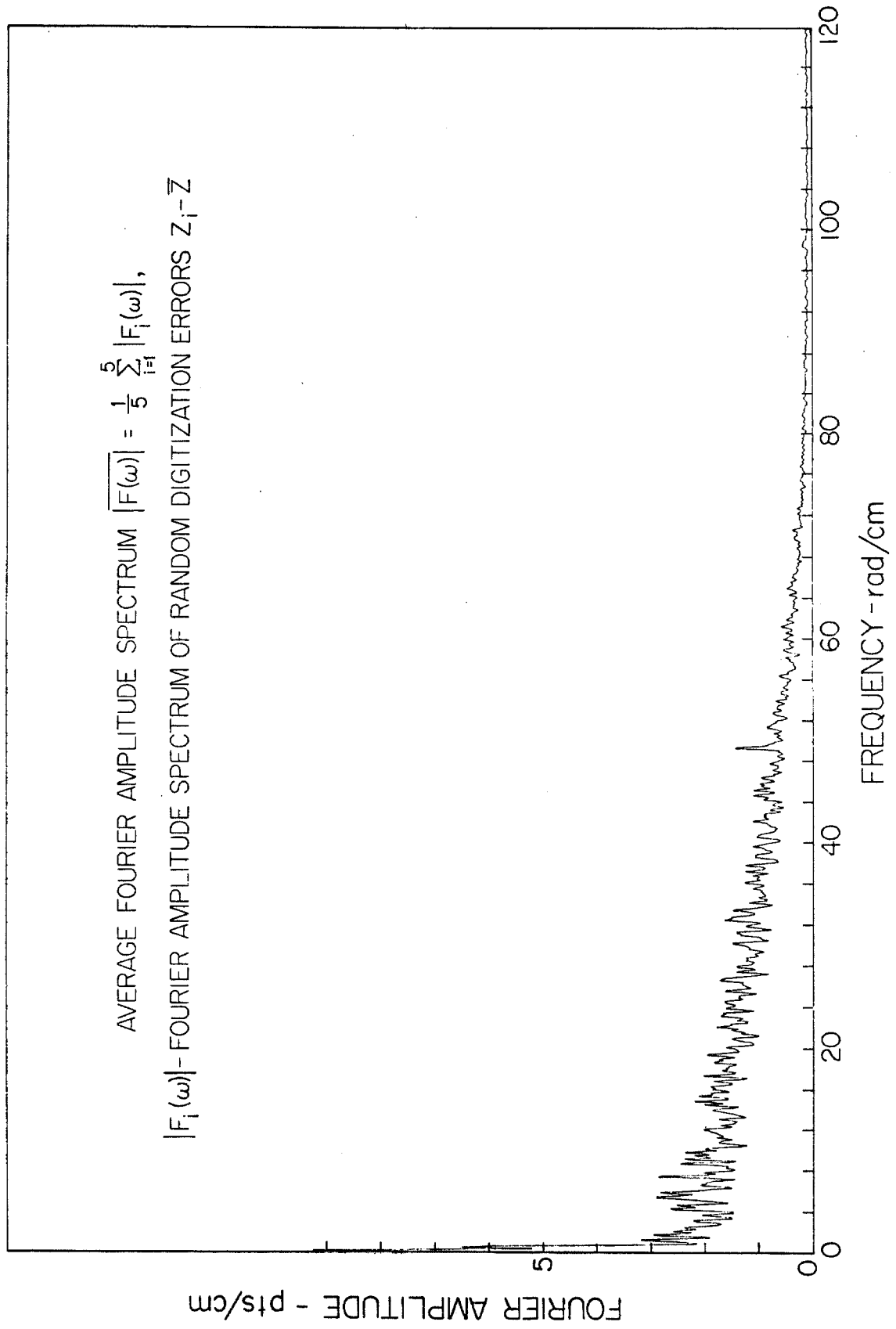
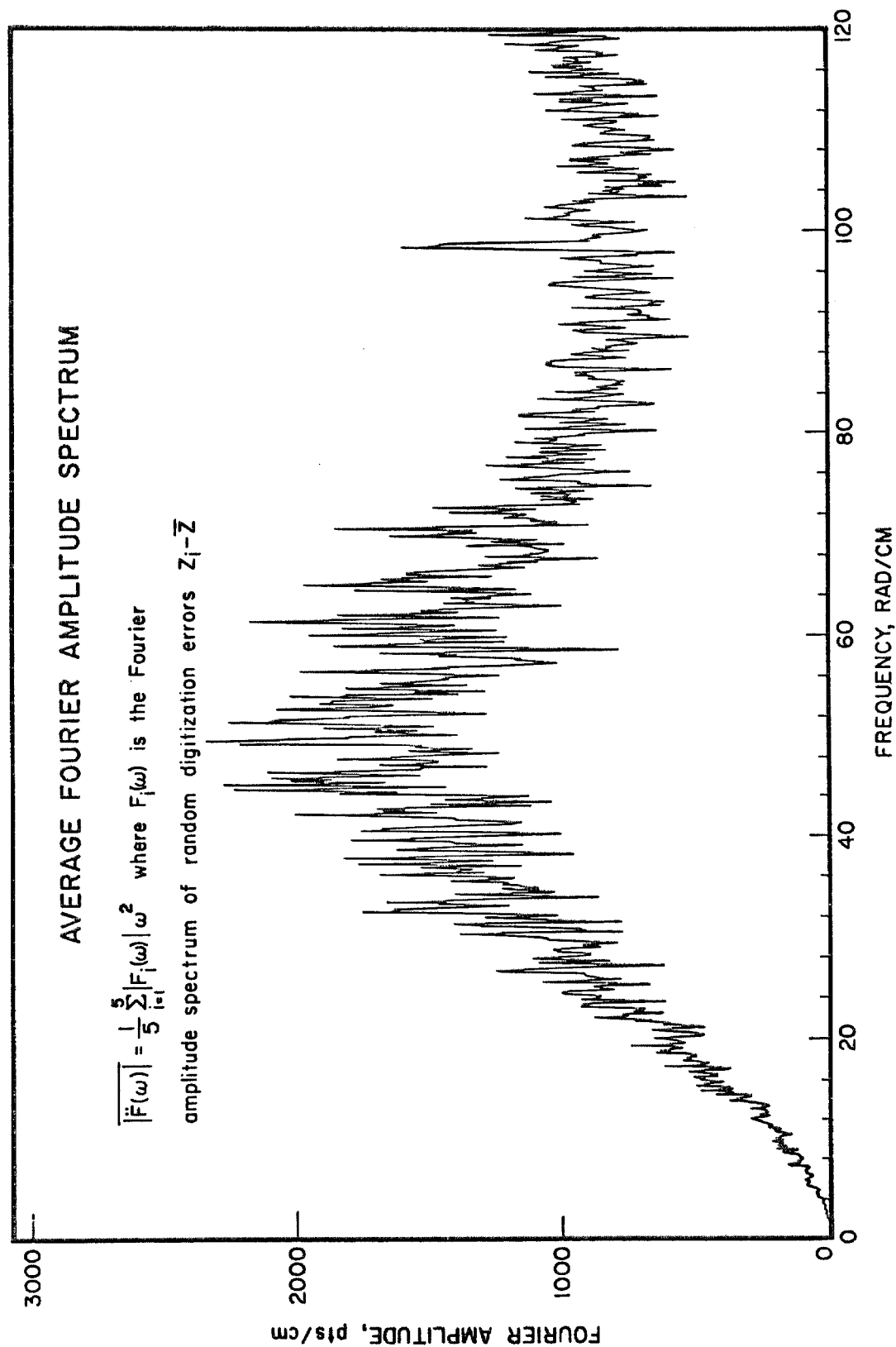AVERAGE FOURIER AMPLITUDE SPECTRUM $\overline{|F(\omega)|} = \frac{1}{5} \sum\limits_{i=1}^{5} |F_i(\omega)|$,

$|F_i(\omega)|$ - FOURIER AMPLITUDE SPECTRUM OF RANDOM DIGITIZATION ERRORS $Z_i - \overline{Z}$

FREQUENCY - rad/cm

FOURIER AMPLITUDE - pts/cm

Figure 5

AVERAGE FOURIER AMPLITUDE SPECTRUM

$$\overline{|\ddot{F}(\omega)|} = \frac{1}{5}\sum_{i=1}^{5}|F_i(\omega)|\,\omega^2 \quad \text{where } F_i(\omega) \text{ is the Fourier}$$

amplitude spectrum of random digitization errors $Z_i - \overline{Z}$

FREQUENCY, RAD/CM

FOURIER AMPLITUDE, pts/cm

Figure 6

SIMPLIFIED PROBABILITY DENSITY FUNCTIONS FOR
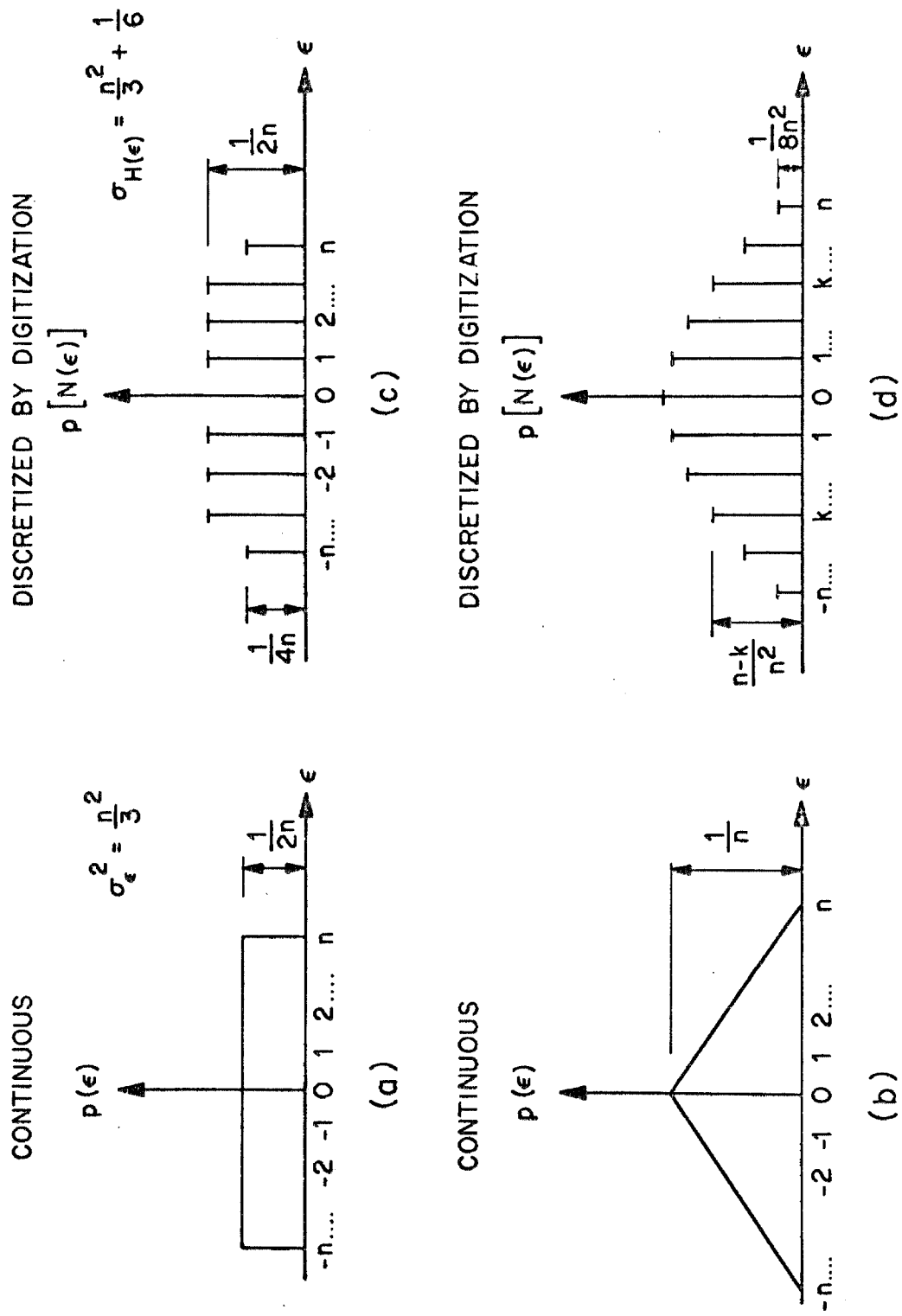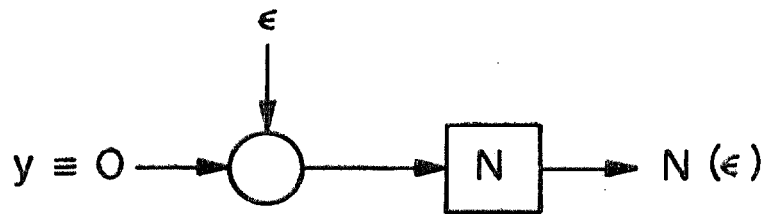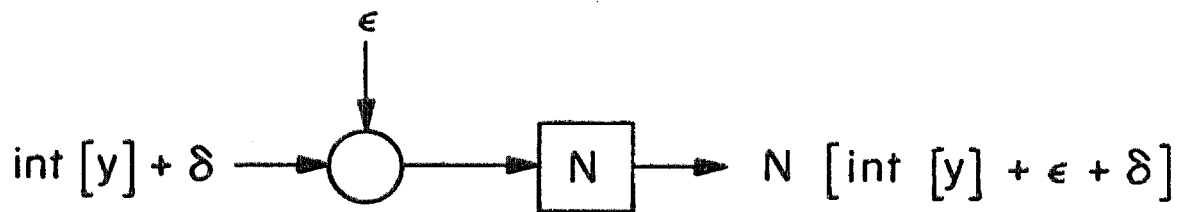THE DIGITIZING ERROR $\epsilon$

Figure 7

# DIGITIZER DISCRETIZATION OPERATOR N



(a)

(b)

Figure 8

that $\sigma^2$ does not necessarily keep increasing with line thickness.

(b) <u>Discretizing error</u>: The digitizer can be described mathematically as an operator N, such that,

$$N(y) = int[y] + H [2(y - int(y)) - 1]$$

where int[y] denotes the integer part of y and H is the unit step operator. The correct value y, at any abscissa x, is read by the operator as $(y + \epsilon)$.

Consider first the case wherein y coincides with a certain digitization level. The probability distribution of $N(\epsilon)$ corresponding to a given $p(\epsilon)$ can then be easily obtained. It may be noted that the new probability distribution is a discrete distribution and that it has a somewhat larger variance than that of $p(\epsilon)$ (Figure 7a and 7b). For the case n = 2, from Figure 7a, the percentage change in the variance due to the presence of the discretizing error (Figure 7c) is only about 13 percent.

If, however, y did not coincide with an exact digitization level, a further error is introduced in the digitization process as seen in Figure 9.

The total error E, in the digitization process becomes,

$$E = N(\epsilon + \delta) - \delta$$

The probability density function $p(\delta)$ depends on the nature of the function being digitized. Assuming that the digitization is done at close intervals along the time axis, $\delta$ can be considered a random, uniformly distributed variable as shown in Figure 10. Knowing $p(\epsilon)$ and $p(\delta)$, $p[N(\epsilon + \delta)]$ can be calculated, and hence the distribution of the error E.
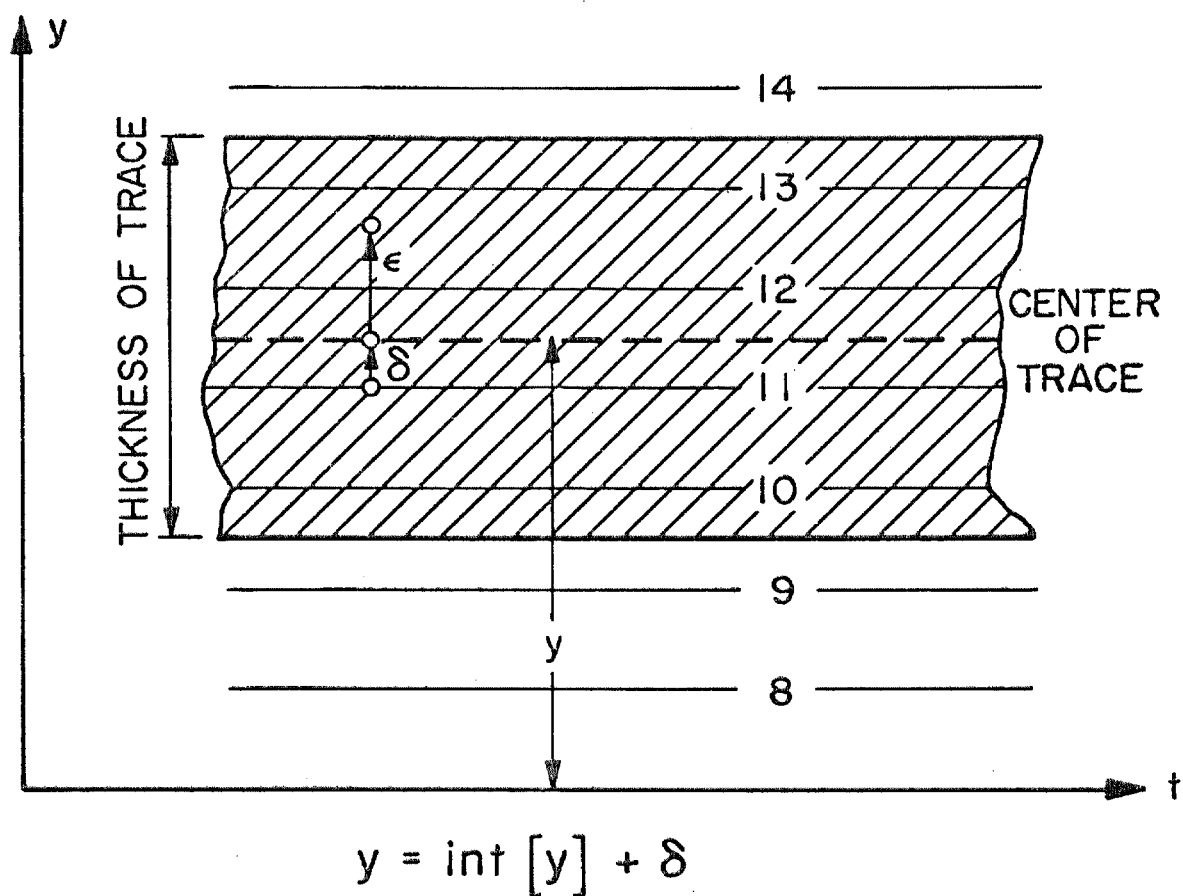
Figure 9. Enlarged portion of a typical optically digitized record
showing the true ordinate y and the recorded ordinate
N (int[y] + ε + δ).

# PROBABILITY DISTRIBUTION $p(\delta)$
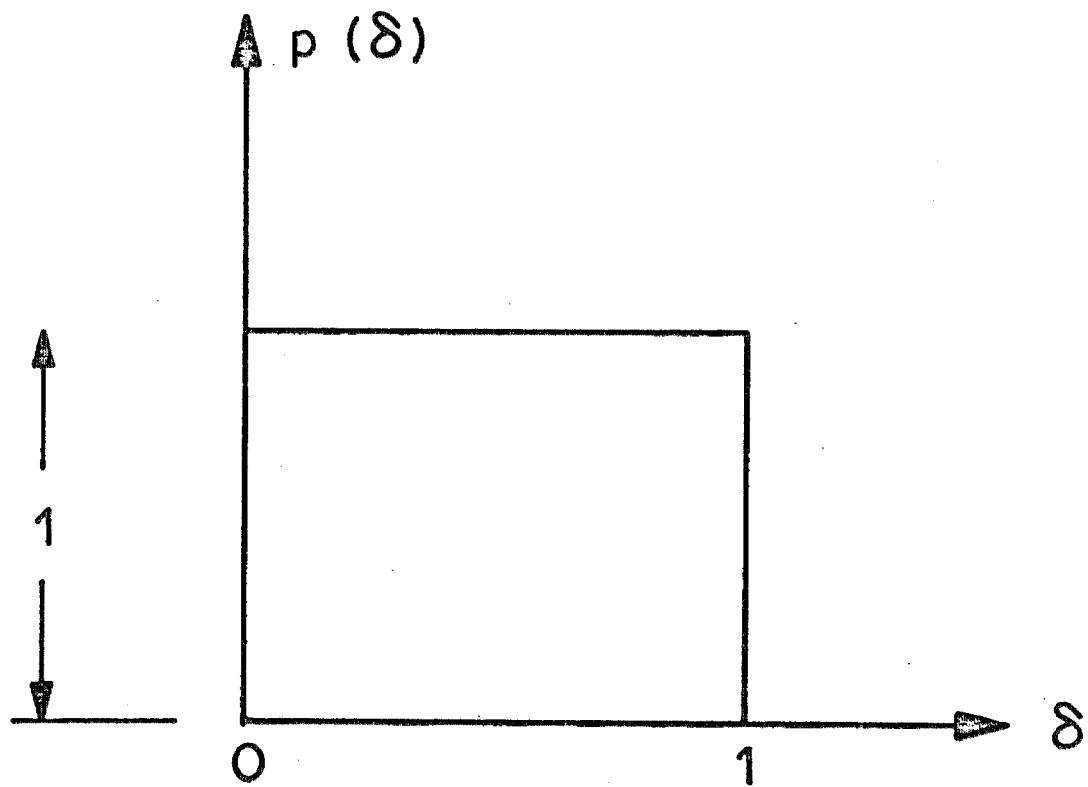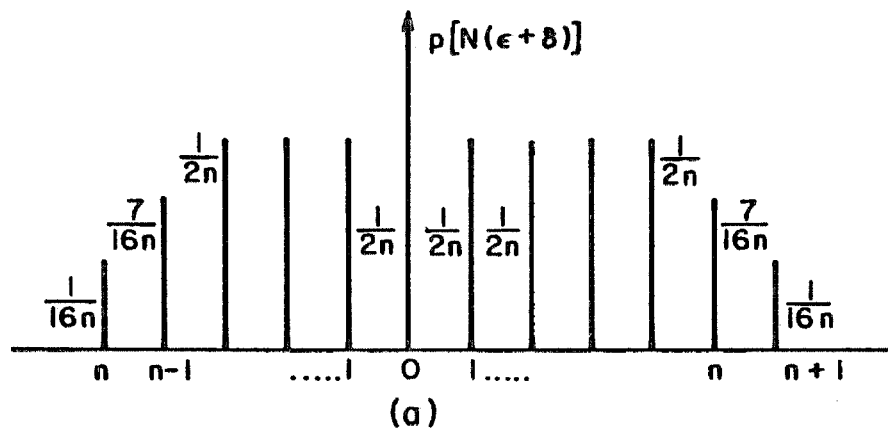## $\delta$ = DIGITIZER TRUNCATION ERROR



Figure 10

To illustrate the effect of $\delta$, we again take $p(\epsilon)$ to be that shown in Figure 7a. The distribution of $p(N(\epsilon + \delta))$ is shown in Figure 11a and that of the error E is shown in 11b. For $n = 2$, the new distribution of Figure 11b has a variance $\sigma_E^2 = \frac{4}{3} + \frac{1}{6} + \frac{1}{12}$. Comparing this with the variance of the error in the case when $\delta \equiv 0$, $\sigma_{N(\epsilon)}^2 = \frac{4}{3} + \frac{1}{6}$, we note that the presence of $\delta$ has increased the variance of the error by only a small amount.

This suggests that the discretizing error, herein represented by the parameter $\delta$ and the function N is not as significant as the human error involved in the digitization process.

4. <u>Inadequate resolution of the digitizing equipment</u>. In this section we shall consider high-frequency errors, which result from the discretization process, and may be the most significant errors in the automatic analog-to-digital conversion process.

To determine the Fourier amplitude spectrum of these errors, an equally spaced sequence was generated in a way that a number is either 1 or -1 so that the probability for both positive and negative values is equal to 0.5. 1000 successive equally spaced, random points were connected by straight lines, thus defining a continuous function (Figure 12). Such a function would result from the digitization of a horizontal straight zero line 30 cm long on a data reducer unit with the resolution interval equal to 2, assuming that there are no human errors in digitization. The Fourier amplitude spectrum $|F(\omega)|$ in pts/cm is plotted versus the frequency $\omega$ on the log-log scale in Figure 13 for the 30 cm long record from Figure 12. From this spectrum we see that the spectral amplitudes of the errors are essentially constant up to the Nyquist frequency $f_N = 16.7$ cycles/cm. When the function to be digitized oscillates, random errors

PROBABILITY DISTRIBUTION $p[N(\epsilon+\delta)]$



(a)

PROBABILITY DISTRIBUTION $p(E)$

$$E = N(\epsilon+\delta) - \delta$$



(b)

Figure 11

- 23 -



Title: SIMULATED DIGITIZATION NOISE



Axis: CENTIMETERS



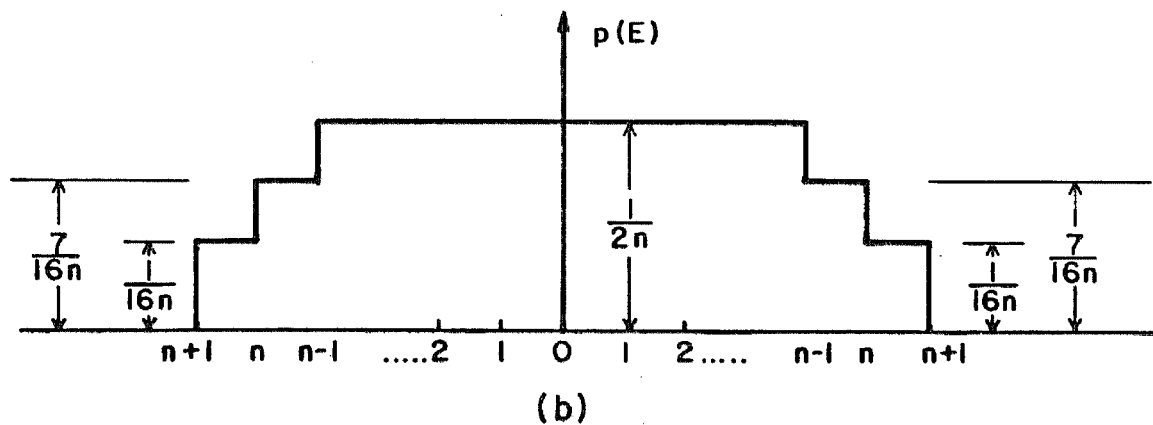ONE RESOLUTION INTERVAL



SIMULATED DIGITIZATION NOISE

CENTIMETERS
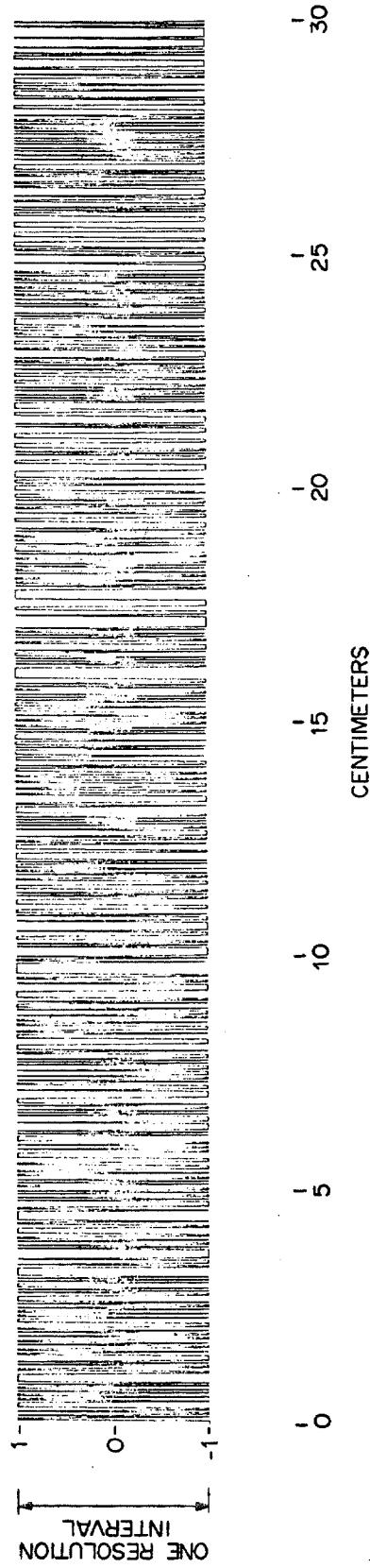
ONE RESOLUTION INTERVAL

Figure 12.    A segment of a typical computer generated trace consisting of an equally spaced sequence of points whose amplitude is either +1 or -1 with equal probability.

FOURIER AMPLITUDE SPECTRUM OF THE
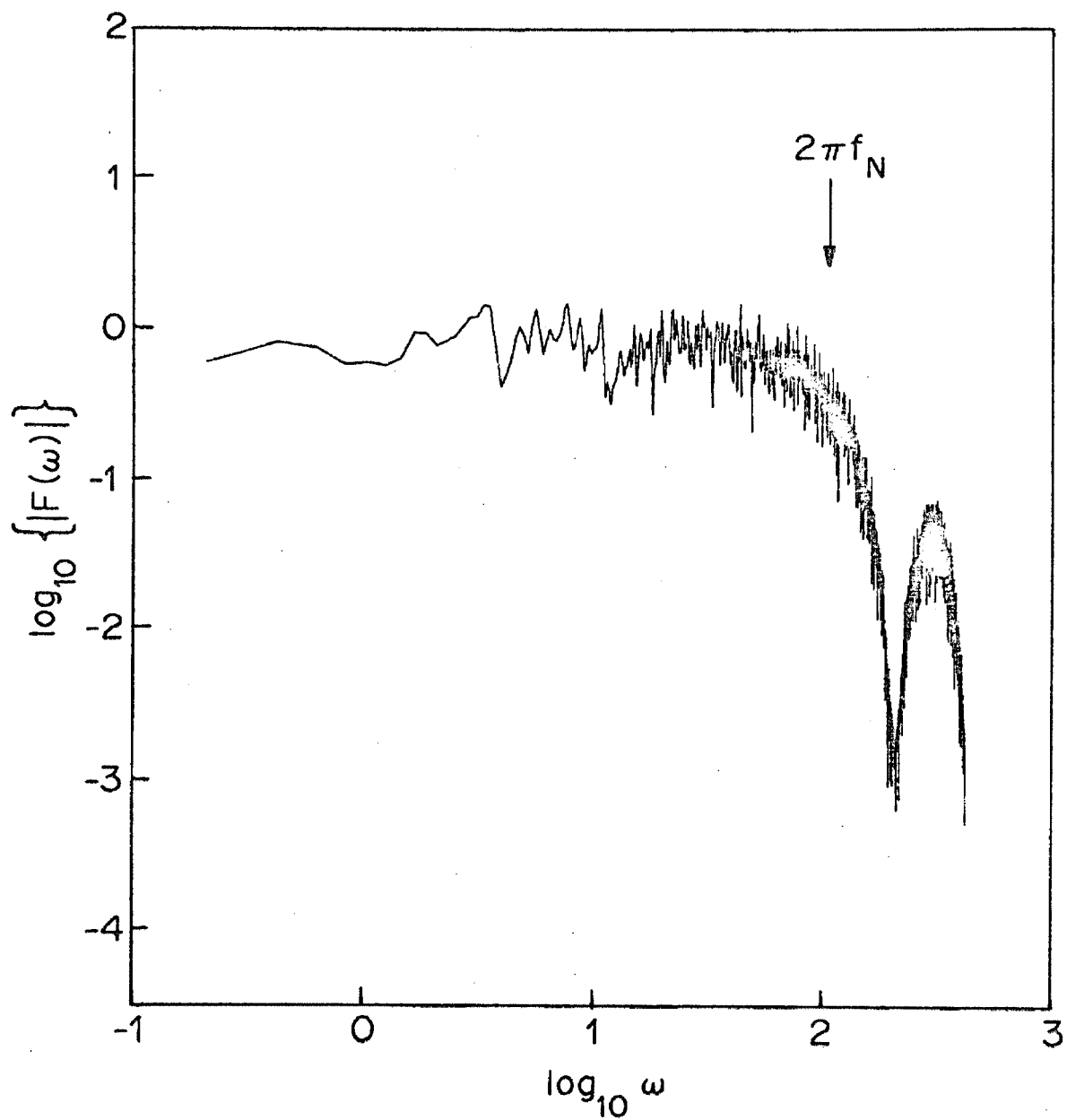SIMULATED DIGITIZATION NOISE

Figure 13

can take on any value between -1 and 1, and equally spaced error

data correspond to white noise with a constant spectrum.

The spectrum in Figure 13 was calculated from 4096 equally spaced

points interpolated to the original 1000 data and interconnected with

straight lines. Thus, the spectrum in Figure 13 also describes the

transfer function corresponding to the process of low-pass filtering

with the decimation and straight-line assumption. The properties of

such low-pass filtering are further examined in the next section.

5. Low-pass filtering effects of the optical-mechanical digitization.

During a typical optical digitization process the operator attempts

to define a continuous function by a sequence of discrete points.

Although the accuracy of the process depends on each individual

operator and the purpose for which the record is to be used, some

general features particularly relevant to accelerogram digitization can

be outlined as follows. While digitizing, the operator choses points

unequally spaced in time according to the frequency of the analog trace.

Thus, for a typical strong-motion accelerogram the density of digit-

ized points tends to increase in higher-frequency portions of the

accelerogram and decrease towards the end of the record. The manner

in which each digitized point is selected is such that the operator

imagines a straight line connecting that and the previous point. Distance

between the two points then becomes a function of the frequency of the

record. The operator always choses the next point so that a straight

line will aptly approximate a section of the continuous analog trace.

Although most modern techniques of digital data analysis do not

define the functional behavior between two digitized points, this has

nevertheless become a common practice in earthquake engineering

and related studies. The assumption of a straight line between the two successive points leads to filtering some small-amplitude high-frequency components that are too small to be detected by the operator, but on the other hand precisely defines the digitized record in the form of a continuous function. Since such digital data are not equally spaced, but are chosen by the operator on the basis of irregularities of the function digitized, fewer points give a better approximation to a continuous function than would equally spaced data of the same density.

To determine the transfer function properties of piecewise straight-line approximation, several cycles of a sine function were defined by equally spaced data interconnected with straight lines. The Fourier amplitude spectrum was then calculated for this continuous function and was divided by the Fourier amplitude spectrum for the exact sine function. This ratio, by definition, gives the modulus of the transfer function for the frequency in question. The result is given in Figure 14, in which the transfer function is plotted versus the number of digitized points per one sine wave cycle. Thus, if the equally spaced digitized data are connected with straight-line segments, the continuous function so defined has essentially the same Fourier amplitudes as the original function up to the Nyquist frequency. Small differences on the order of a few percent for 5 to 10 points per cycle gradually increase to about 20 percent near the Nyquist frequency, corresponding to 2 points per cycle.

This experiment with equally spaced points was performed to approximately determine the shape of the transfer function that would correspond to the unequally spaced points of the same average density. The validity of such an approximation was experimentally verified by
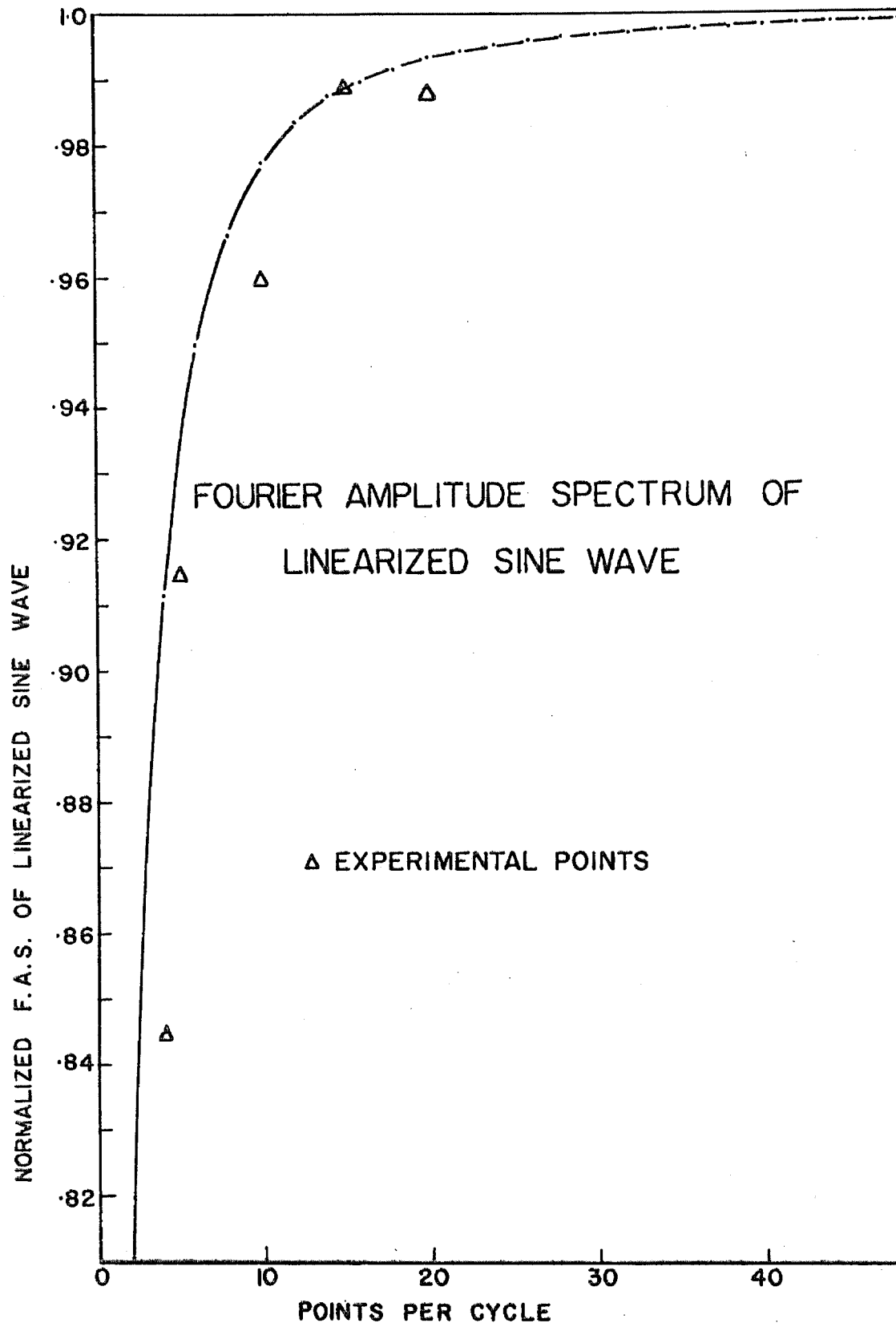
Figure 14.   A comparison of the theoretically determined Fourier
             amplitude spectrum of a linearized sine wave (—·—·)
             and the experimentally obtained spectrum ($\triangle$).

optically digitizing several sine wave traces and using unequally
spaced data of various densities. The transfer functions were cal-
culated in the same way as for the equally spaced points, and the
result is indicated in Figure 14 by triangular points. From the
agreement of experimental points for digitized, unequally spaced
data and the theoretical curve, we conclude that by assuming a straight
line between points the transfer function for the unequally spaced
optical digitization process may be described by the curve given in
Figure 14.

## The Minimum Average Period in Hand Digitized Accelerograms

The density of digitized points naturally varies from one operator
to another. This is illustrated in Figure 15, where the average number
of the digitized points per one cycle is plotted versus period. The
least-square-fitted straight lines show the expected tendency towards
the increase in the number of points for longer periods. Certain
distinct features of these curves distinguish this kind of hand digitized
data from equally spaced hand or machine digitization. For equally
spaced data these curves would intersect the origin. As an example,
a dashed line is plotted corresponding to the $\Delta t = 0.1$ sec. Such a line
intersects the level of 2 points per cycle at the period of 0.2 seconds
in agreement with the Nyquist frequency, for this case equal to 5 cps.
On the other hand the lines calculated for the four typical acceleration
digitizations with the unequally spaced data never go below the level of
2 points per cycle.

Figure 16 gives the histogram of the lowest average period
present in the early 48 (Hudson et al 1969) hand-digitized paper records.

SCATTER OF POINTS PER CYCLE
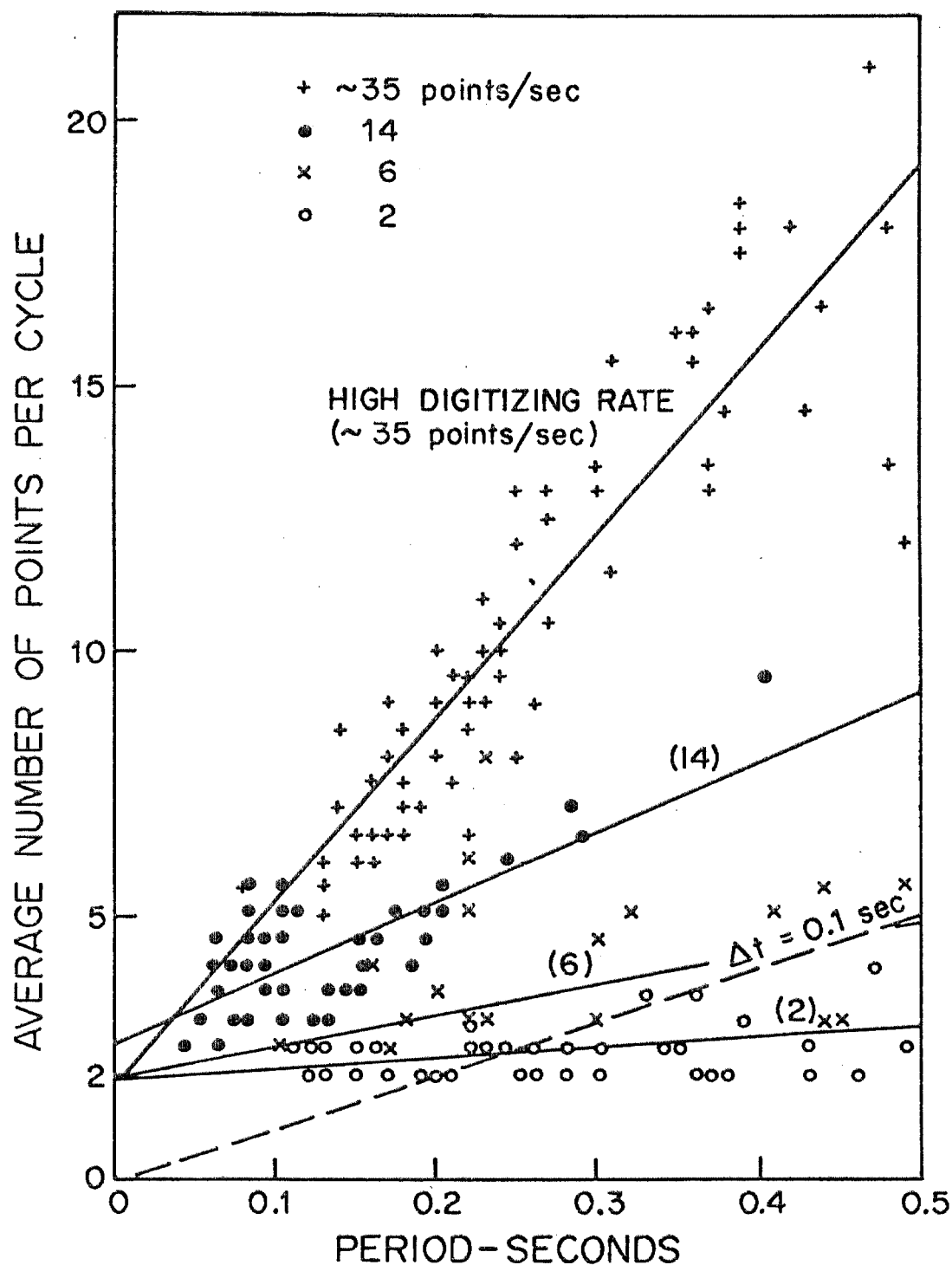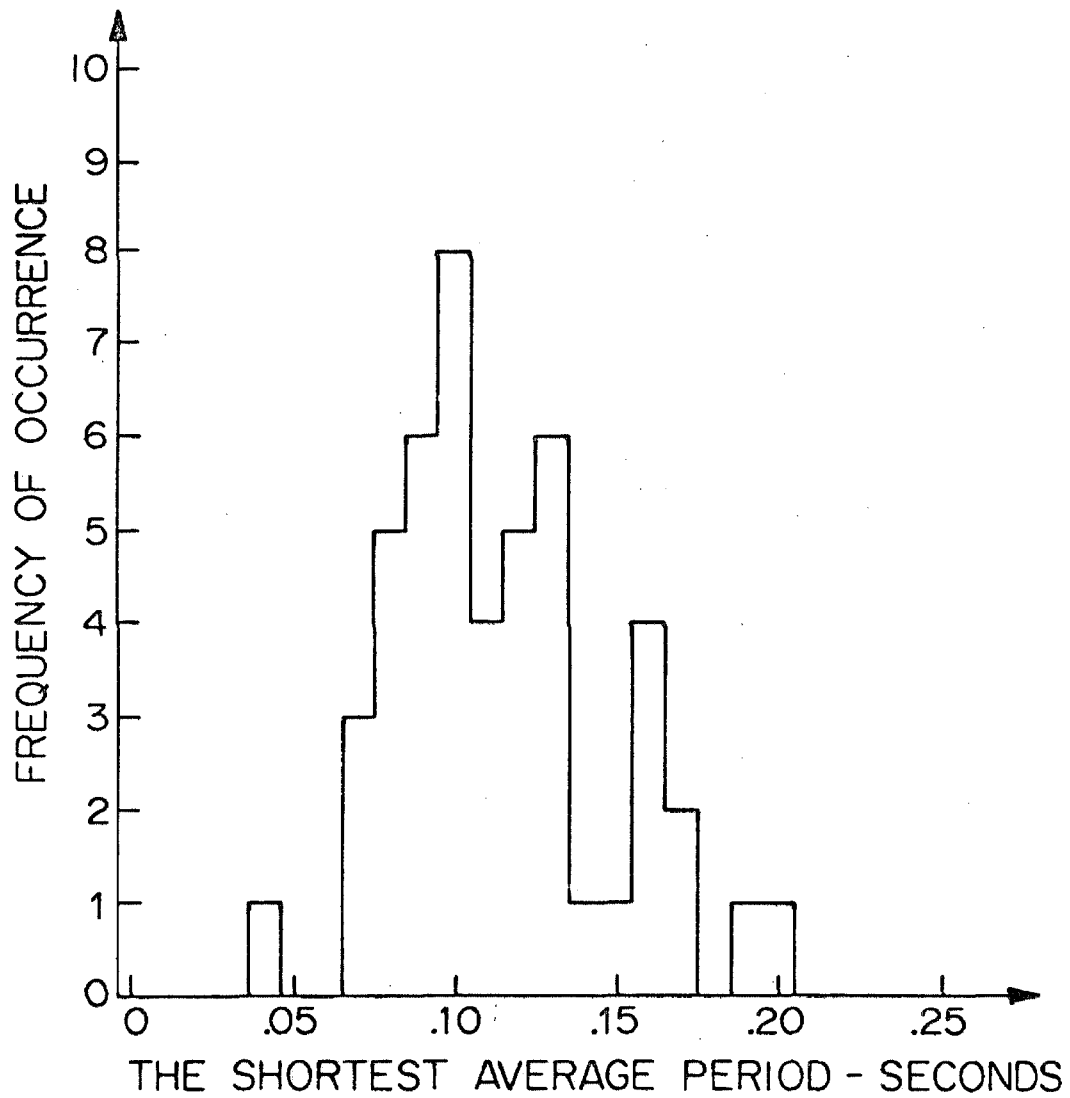AND SECONDS PER CYCLE IN EVERY SECOND
OF FOUR TYPICAL RECORDS

Figure 15

Figure 16

From this histogram we observe that the lowest average period picked over one record may in many cases be greater than 0.04 seconds corresponding to the frequency of 25 cps. Because this histogram was obtained on the basis of data averaged over one second and the operator's own judgement, of the number of points to be digitized according to the local frequency content, the highest frequency actually resolved in a short segment of the record is substantially above average. Approximately 150 additional paper records recently hand-digitized contain on the average about 40 points per second and are well represented by the steepest curve in Figure 15. For these records the average Nyquist frequency is about 20 cps. It, therefore, appears that most of the hand-digitized paper accelerograms contain information on the frequencies near and above the 20 cps. Figure 17 gives a histogram of the occurrence of the average interval of digitization and is compiled from 263 different components.

Fundamental frequencies of most instruments fall between 10 and 30 cps. Recorded signals with frequencies higher than 30 cps would either have a very low signal-to-noise ratio or be distorted by the higher modes of vibration of the instrument transducers, or have both effects present. We therefore conclude that the highest frequency that can be extracted from hand-digitized paper records is about 25 cps. This high-frequency limit is, of course, the consequence of presently available and practical means for hand-digitization and processing of paper records. With future improvements in instrument design and in the technology of data processing, this frequency will no doubt be further increased.
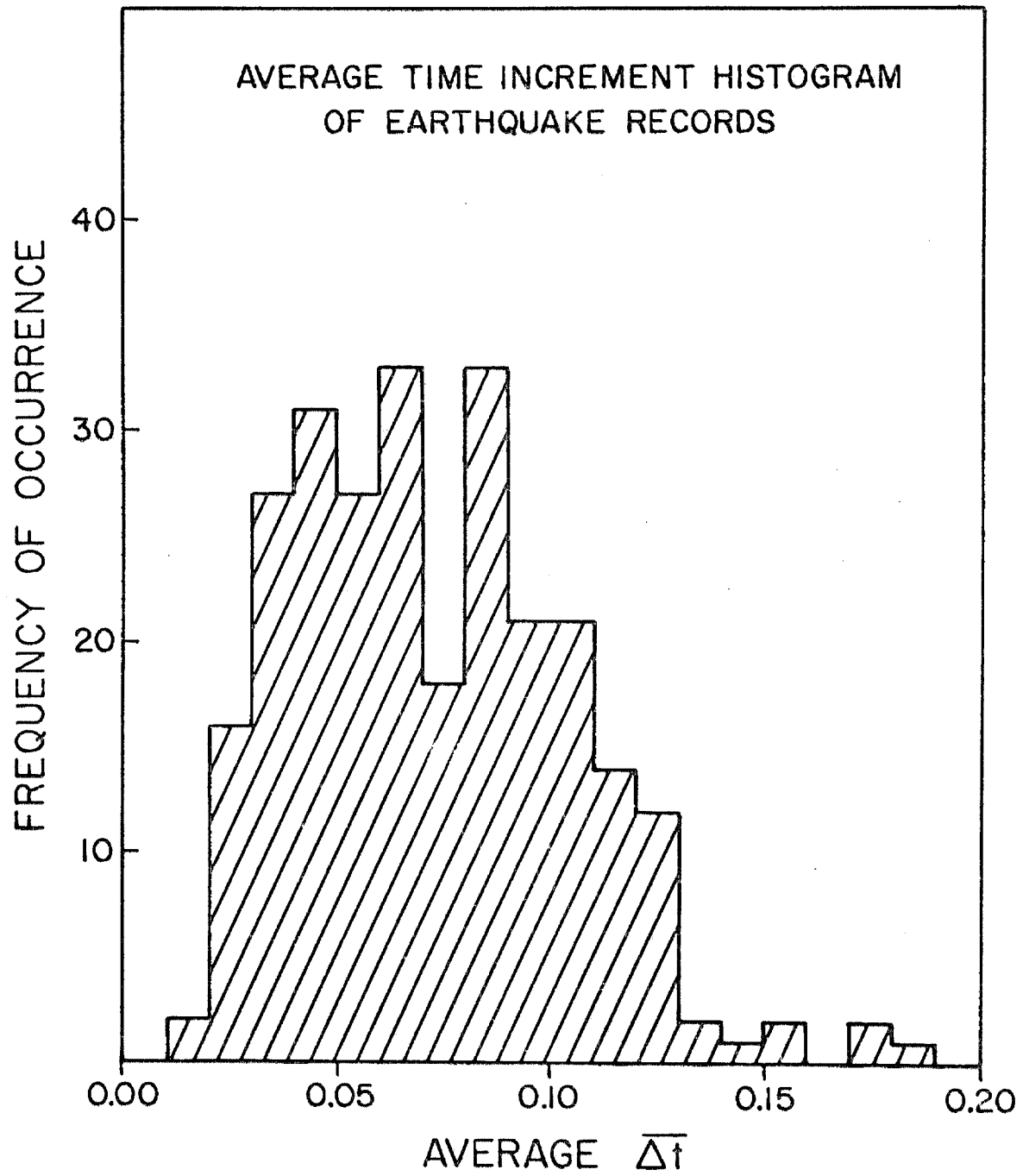
Figure 17

# INSTRUMENT CORRECTION

From Figure 1 it may be concluded that for the natural frequencies of acceleration transducers between 10 and 30 cps, the recorded instrument response may be taken to represent ground accelerations up to frequencies of about 5 to 10 cps, respectively. To accurately recover higher frequencies, an instrument correction must be performed.

In this work we will neglect errors resulting from imperfections in the transducer design. This is permissible because the routine optical-mechanical digitization process does not resolve frequencies higher than about 25 cps, and imperfections in the transducer design affect seriously only the higher frequencies. In the future, analog magnetic tape recordings will be digitized electronically with equally spaced data at much greater rate than is presently feasible with the optical digitization process; however, transducers will have to be designed to eliminate all the higher translational and torsional modes of vibration to permit retrieval of the high-frequency signals.

The high-frequency limit to which accurate accelerations may be recovered is determined by the lower of the two characteristic frequencies. One of these frequencies corresponds to the highest frequency defined by the digitized data. This is $f_N$ if the data are equally spaced, or the equivalent highest frequency resolved by unequally spaced data in the sense of Figure 16. The other characteristic frequency is obtained by the intersection of the instrument response curve (Figure 1) and the chosen constant multiple of the digitization noise level (Figure 13). The latter level may depend on the accuracy

required of the corrected data and the particular characteristics of the instrument response curve. Since the natural frequency of the typical acceleration transducer is between 10 and 30 cps for all earthquake accelerograms, the first frequency, governed by the digitization rate, becomes important for all strong-motion accelerograms presently analyzed. The low-pass filtered accelerograms then have to be corrected for instrument response. Two different methods of making this correction that lead to the same result are presented.

## Differential Equation Approach

In this approach to instrument correction of a recorded accelerogram, use is made of a differential equation describing the behavior of a single degree of freedom oscillator, viscously damped.

$$\ddot{x} + 2\omega_o \zeta_o \dot{x} + \omega_o^2 x = -a \qquad (1)$$

In this equation,

$x$ = relative motion of the transducer mass

$\omega_o$ = natural frequency of the transducer ($\omega_o = 2\pi f_o$)

$\zeta_o$ = fraction of critical damping

$a$ = absolute ground acceleration.

When such a transducer is used as an accelerometer $\omega_o$ has to be a large number (normally about 100 and larger) so that only the term $\omega_o^2 x$ is significant on the left-hand side of the equation and terms $\ddot{x}$ and $2\omega_o \zeta_o \dot{x}$ may be neglected. As may be seen this approximation is adequate as long as recorded frequencies are significantly smaller than $\omega_o$, and in that case ground acceleration a is approximately given by

$$a \approx - \omega_o^2 x \qquad\qquad (2)$$

In order to extend accurately the information about ground acceleration to the higher frequencies, all terms on the left hand side of the equation (1) have to be considered, requiring differentiation of the recorded instrument response x. As is well known, this may lead to serious difficulties because such a process would amplify high-frequency digitization errors. In a recent study Trifunac and Hudson (1970) demonstrated that such difficulties may be avoided if digitization errors are filtered out prior to the differentiation process. This is, of course, based on the assumption that high-frequency digitization errors are well above recorded high-frequency components of ground motion, or if not, that the filtering of some of the real high-frequency components of ground motion does not seriously affect the quality of the digital data. Since the predominant frequencies of digitization errors are closely related to the average interval of digitization, it follows that one should try to digitize as many closely spaced points as possible.

High Frequency Mathematical Oscillator Response

As mentioned in the previous section, if the natural frequency of the transducer $\omega_o$ can be sufficiently high, ground motions of smaller frequencies are approximately recorded as acceleration and are given by the equation (2). As mentioned above, the natural frequency $\omega_o$ for most accelerographs presently operating is between 10 cps and 30 cps. These relatively low frequency values result from the considerations in transducer design and the instrument amplification required. Since the validity of recorded transducer motion as ground acceleration in

the higher-frequency domain depends mainly on the high numerical value of $\omega_o$, we shall demonstrate here how one can construct the response of a high-frequency single degree of freedom oscillator, viscously damped, by using the recorded instrument response as an input. This approach is merely an extension of a method given by McLennan (1969).

Let X be the relative response of an accelerograph with natural frequency $\omega_o$ and fraction of critical damping $\zeta_o$. Equation (1) is then rewritten as

$$\ddot{X} + 2\omega_o \zeta_o \dot{X} + \omega_o^2 X = -a \tag{3}$$

and equation (2) as

$$\omega_o^2 X \approx -a \tag{4}$$

The response of any oscillator with a frequency $\omega$ and fraction of critical damping $\zeta$ is given by

$$\ddot{x} + 2\omega \zeta \dot{x} + \omega^2 x = -a \tag{5}$$

Using equation (4) the approximate response $x_a$ of the same oscillator would be given by

$$\ddot{x}_a + 2\omega \zeta \dot{x}_a + \omega^2 x_a = \omega_o^2 X \tag{6}$$

Combining equations (3) and (5), assuming zero initial conditions, and taking the Laplace transform we get

$$x(s) \left[ s^2 + 2\omega \zeta s + \omega^2 \right] = X(s) \left[ s^2 + 2\omega_o \zeta_o s + \omega_o^2 \right] \tag{7}$$

which, as suggested by McLennan (1969), can be rewritten as

$$x(s) = X(s) + \frac{2(\omega_o \zeta_o - \omega \zeta) s X(s)}{s^2 + 2\zeta \omega s + \omega^2} + \frac{(\omega_o^2 - \omega^2) X(s)}{s^2 + 2\zeta \omega s + \omega^2} \tag{8}$$

The Laplace transform of equation (6) gives

$$x_a(s) = \frac{\omega_o^2 X(s)}{s^2 + 2\zeta\omega s + \omega^2} \tag{9}$$

and

$$\dot{x}_a(s) = \frac{\omega_o^2 s X(s)}{s^2 + 2\zeta\omega s + \omega^2} \tag{10}$$

Combining equations (9) and (10) with equation (8) and transforming back to the real time space one obtains

$$x(t) = X(t) + \frac{2(\zeta_o \omega_o - \zeta\omega)}{\omega_o^2} \dot{x}_a(t) + \frac{(\omega_o^2 - \omega^2)}{\omega_o^2} x_a(t) \tag{11}$$

Since this equation gives the exact response x(t) for an oscillator with frequency $\omega$ and damping $\zeta$ as a combination of the instrument response X(t) and the approximate response $x_a(t)$ and $\dot{x}_a(t)$, McLennan (1969) proposed to use this equation to obtain the exact response spectrum.

Although it is important to have the exact spectra of recorded ground motion, it is more important to determine the exact ground acceleration so that it can be used as an input to any dynamic response calculations. It is proposed here to use equation (11) to determine the response of an oscillator for which $\zeta = 0.707$ and $\omega \gg \omega_o$; $\omega^2 x(t)$ then becomes an excellent approximation to a(t). Although this approach does not explicity involve numerical differentiation of the function X(t), it amplifies the high-frequency errors introduced into the X(t) through the optical-mechanical digitization process. Therefore, like the method based on the differential equation of the instrument transducer, this approach may be used only after random digitization errors have been filtered out from the digitized accelerogram.

## Instrument Correction Procedures - A Case Study

A typical, recorded, strong motion accelerogram (Figure 18) was taken to be the exact acceleration a(t) and was used to calculate the response of an oscillator with $\omega_o$ = 6.28 rad/sec. and $\zeta_o$ = 0.60. Equation (3) was integrated using the third order Runge-Kutta method. The computed relative displacement response is given in Figure 19. It was then assumed that only the relative displacement response in Figure 19 was known, and the two methods outlined above were used to correct this response and derive the original input acceleration.

The calculated response in Figure 19 was optically digitized on the Benson Lehner 099D datareducer with 1294 unequally spaced data points. These data represent the uncorrected "accelerogram" $X_1(t_i)$ (Figure 20) as a typical basic input. The next step was to interpolate the equally spaced 200 pts/sec to the record $X_1(t_i)$, which gave $X_2(n\Delta t)$ with $\Delta t$ = 0.005 sec. This equally spaced "accelerogram" was then used as an input to the digital Ormsby filter. The details on the use of the digital Ormsby filter may be found in our previous report (Trifunac 1970). For $\Delta t$ = 0.005 sec and 200 filter weights symmetrically distributed over the filtering interval of 1 sec, the resulting filter transfer function is as in Figure 21.

For this particular example we chose to analyze a typical case for which the characteristic high frequency cutoff is determined by the digitization noise level, far beyond the instrument natural frequency, here chosen as 1 cps. We believe that such an example illustrates how far instrument corrections can be applied to recover the input acceleration beyond the natural frequency of the transducer. In particular, this example shows that with careful digitization, the "displacement meter"
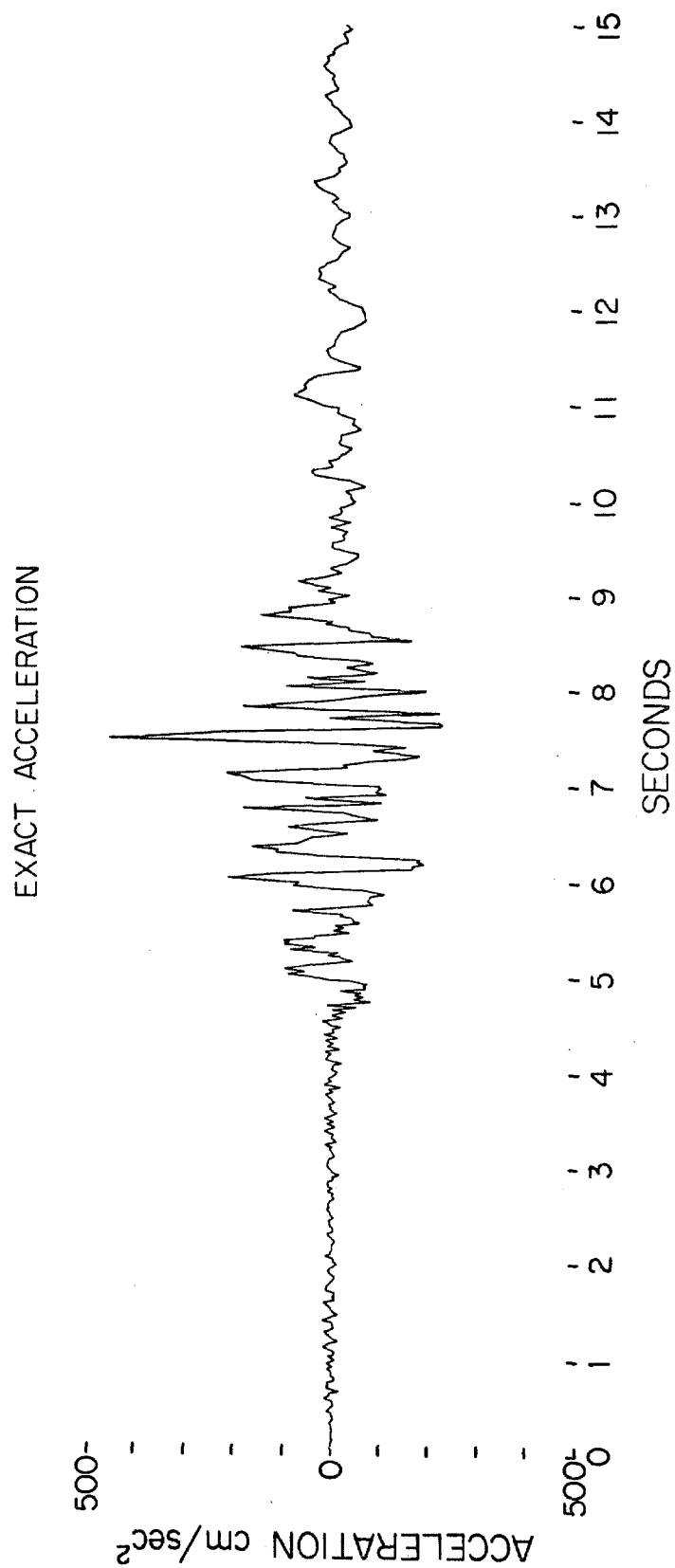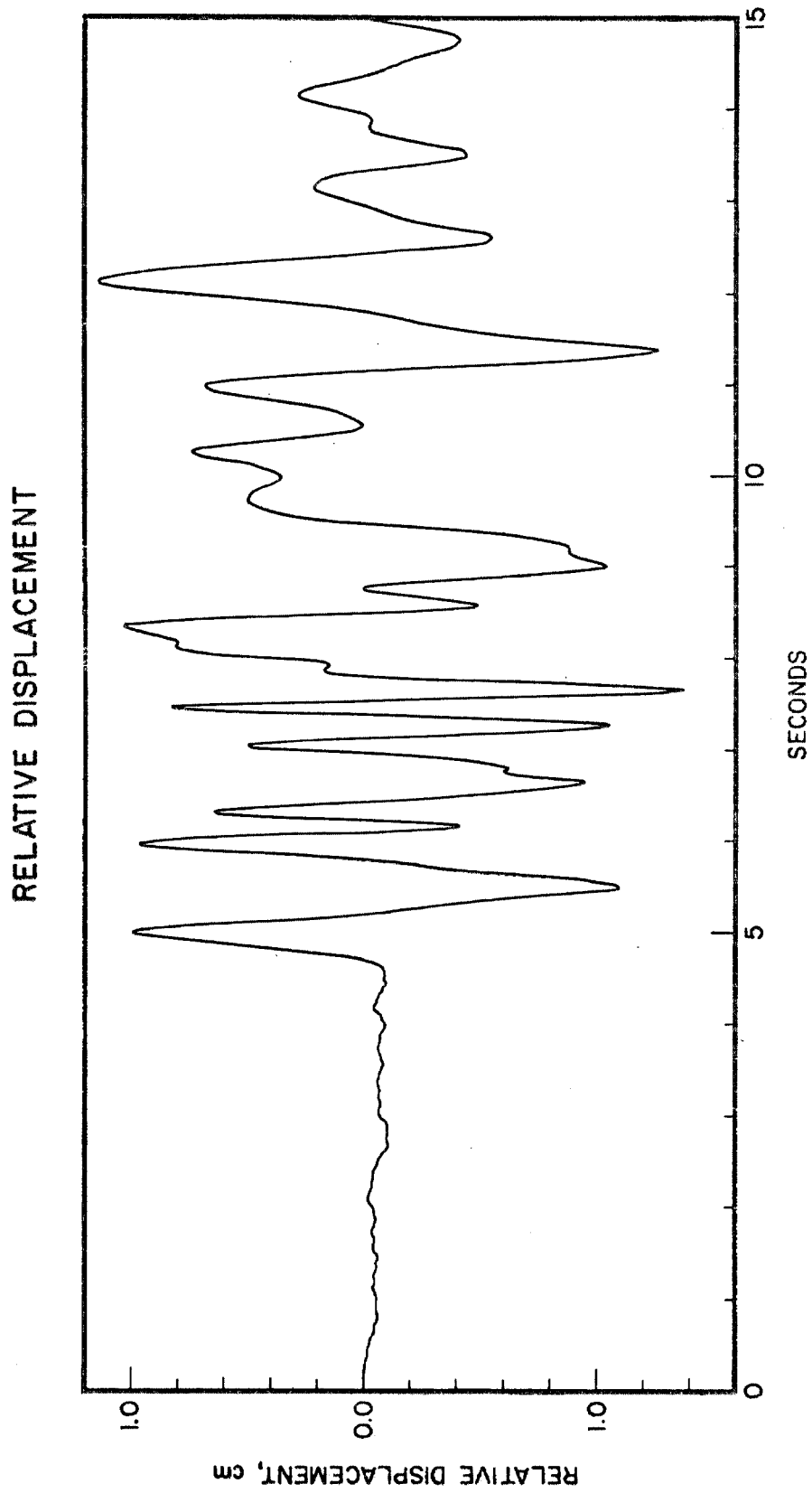
Figure 18

RELATIVE DISPLACEMENT



Figure 19

FLOW CHART FOR ACCELEROGRAM INSTRUMENT CORRECTION

INPUT

Uncorrected accelerogram $X_1(t_i)$

① 

Interpolate equally spaced data $X_2(n\Delta t)$

②

Low pass filter $X_2(n\Delta t)$ by using Ormsby filter

$f_c$ cps

$X_3(n\Delta t)$

either

**Differential Equation Approach**

③ differentiate $X_3(n\Delta t)$ to get $\dot{X}_3(n\Delta t)$ and $\ddot{X}_3(n\Delta t)$

④ Use differential equation to construct accelerogram
$a(n\Delta t) = -\ddot{X}_3(n\Delta t) - 2\omega_0\zeta_0\dot{X}(n\Delta t) - \omega_0^2 X(n\Delta t)$

OUTPUT $a(n\Delta t)$

**or**

**High Frequency Oscillator Approach**

③ Use $\omega_0^2 X_3(n\Delta t)$ to calculate $x_d(n\Delta t)$ and $\dot{x}_d(n\Delta t)$ for oscillator with $\omega \gg \omega_0$ and $\zeta = 0.707$

④ Construct corrected accelerogram
$a(n\Delta t) = -\omega^2 \left[ X_3(n\Delta t) + \dfrac{2(\zeta_0\omega_0 - \zeta\omega)}{\omega_0^2} \dot{x}_d(n\Delta t) + \dfrac{(\omega_0^2 - \omega^2)}{\omega_0^2} x_d(n\Delta t) \right]$

OUTPUT $a(n\Delta t)$

Figure 20

TRANSFER FUNCTION FOR ORMSBY FILTER

FREQUENCY, CPS
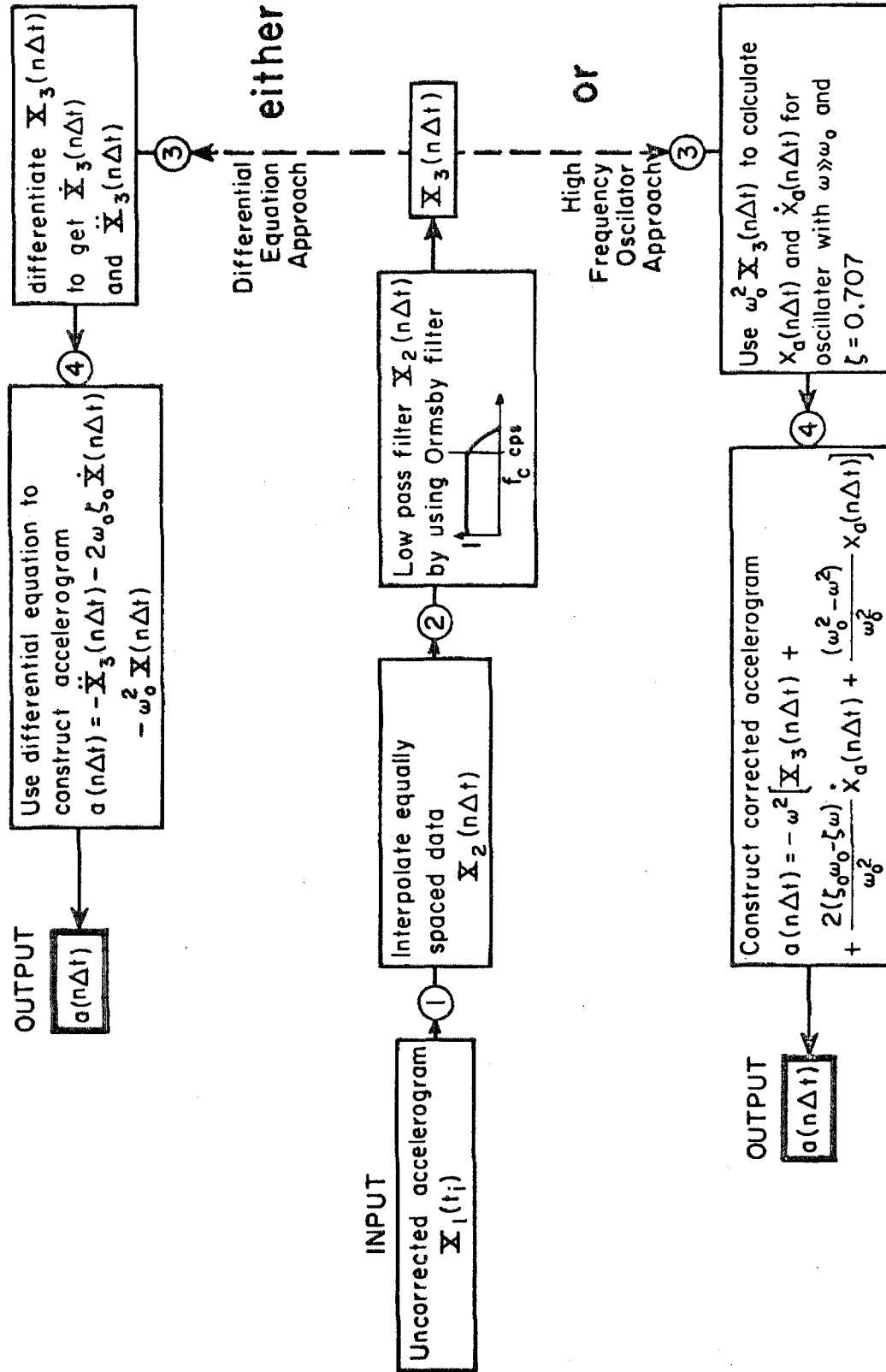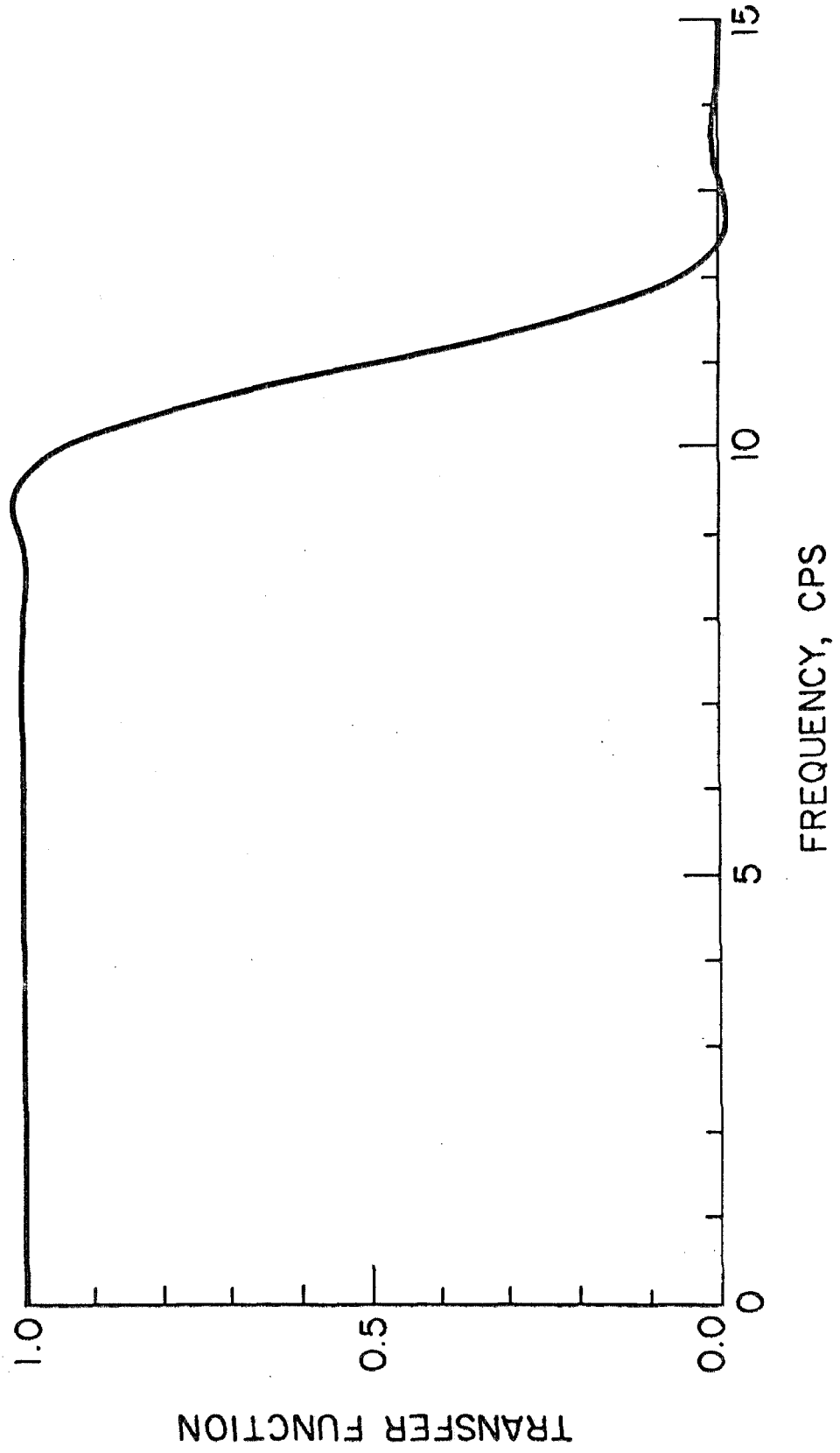
TRANSFER FUNCTION

Figure 21

output can be used to recover input acceleration to a frequency as much as an order of magnitude higher than the natural frequency of the transducer.

The recorded amplitudes in Figure 19 are of the order of 1 cm and the accuracy of the digitization is estimated to be about (1/1000) cm. If we decide to accept a signal-to-noise ratio of about 10, the critical tenfold noise level is then about (1/100) cm. For the transducer natural frequency of 1 cps and the single-degree-of-freedom system, this means that we can use the digitized data to about 10 cps. We have, therefore, chosen 10 cps as the roll-off frequency for the Ormsby low-pass filter in this case.

The low-pass filtered "accelerogram" $X_3(n\Delta t)$ was processed in two ways (Figure 20). First, $X_3(n\Delta t)$ was differentiated two times using a centered difference scheme, and the differential equation method was used to construct the input acceleration for $\omega_o = 6.28$ rad/sec and $\zeta_o = 0.60$. The result is given in Figure 22. Second, the low-pass filtered "accelerogram" $X_3(n\Delta t)$ was multiplied by $\omega_o^2$ and used as an "approximate acceleration" to calculate the approximate response of a single-degree-of-freedom oscillator with $\omega = 30$ cps and $\zeta = 0.707$. The approximate relative velocity $\dot{x}_a$ and displacement $x_a$ were then used in equation (11) to determine the exact response (Figure 20) and thus derive the input acceleration approximately given by $\omega^2 x(t)$ (Figure 22). As may be seen in Figure 22, both results are essentially identical. When a comparison is made with the original input acceleration plotted on the top of Figure 22, it becomes obvious that as the consequence of the low-pass filtering procedures, some of the high frequency components higher than 10 cps are not present in the
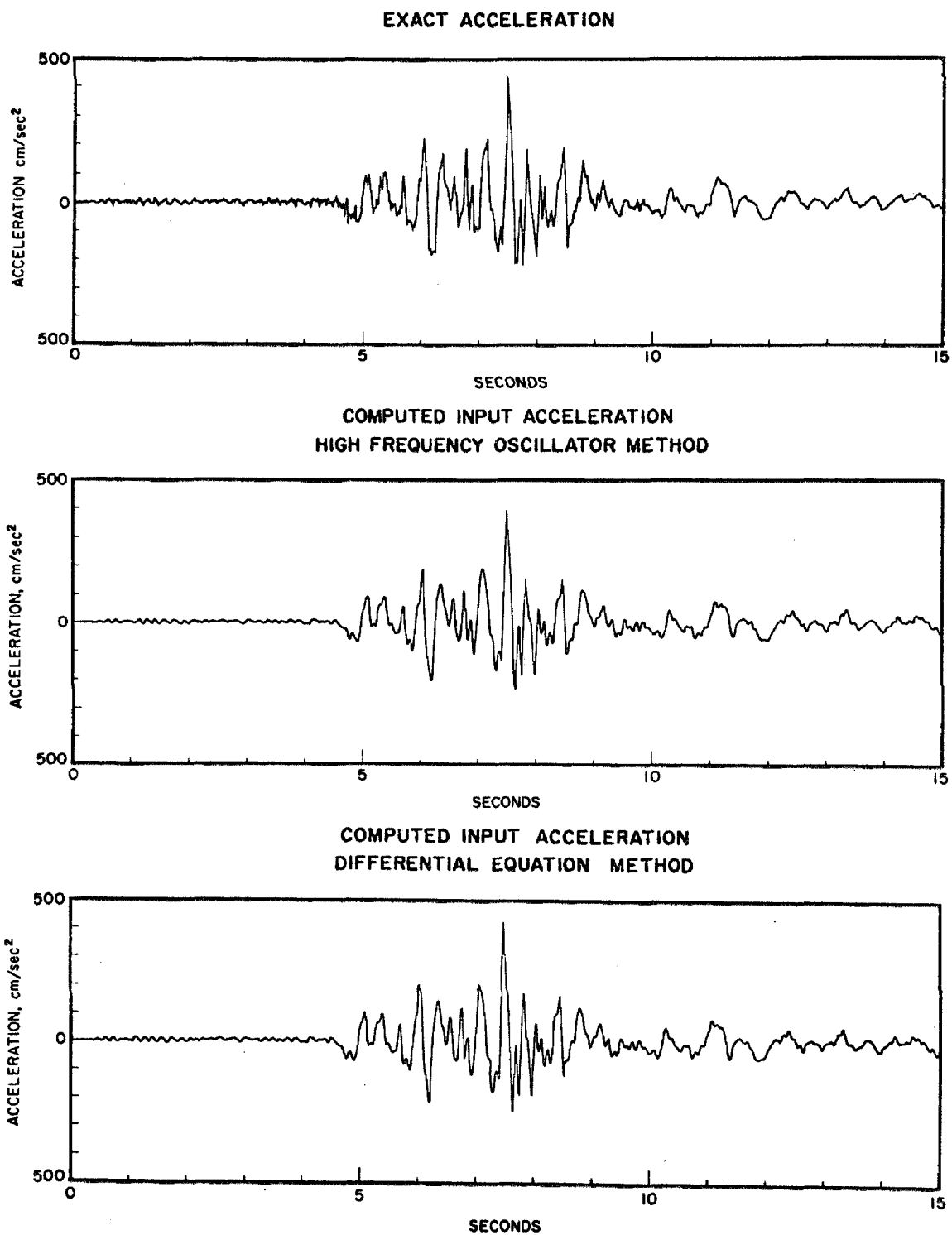
Figure 22

reconstructed accelerograms. Nevertheless, the general agreement between exact input acceleration and reconstructed acceleration is excellent.

The main purpose of this parallel outline of the two methods is to demonstrate the accuracy and to offer two alternate ways of arriving at the same result. In our opinion, however, the method using the differential equation of the instrument is preferable because of its simplicity. The method based on the high-frequency oscillator is equally applicable and accurate, but may cause some difficulties if $\omega$ is taken to be too large and if only single precision accuracy is used for computations. This is because for a large $\omega$ the terms $(1 - \frac{\omega^2}{\omega_o^2})x_a$ and X in equation (11) are nearly the same and of opposite sign, so that the truncation errors may become catastrophic.

An instrument with a natural period of 1 sec was chosen to demonstrate the power of the instrument correction methods outlined above. These methods can also be applied to any transducer output and are not restricted to the simple single-degree-of-freedom oscillators with relative displacement outputs used here. This example clearly shows how it is still possible to recover significantly high frequency components of the exact input acceleration from the relatively smooth response in Figure 19.

## CONCLUSIONS

Our investigation of high-frequency errors in hand-digitized paper accelerograms and the procedures for the accelerometer response correction may be summarized as follows:

1. The analysis of the variance of errors resulting from the accelerogram line thickness, human reading error, digitizer truncation error, and the digitizer discretization error shows that for typical line thickness and a digitizer unit with a resolution 1/300 cm or better, the human reading error is the main contributing factor to the variance of error.

2. Random digitization errors consisting of all the above-mentioned errors and including parallax are nearly normally distributed with the mean centered on the accelerogram trace centerline and the average standard deviation equal to about 1/300 cm.

3. The frequency transfer function associated with the process of decimation of equally spaced data and the subsequent connection of the resulting points with a straight line is essentially equal to unity up to the Nyquist frequency for the final sampling rate.

4. Most hand-digitized paper accelerograms contain locally reliable information on the frequencies near and above 25 cps. Therefore, the highest frequency defined by the equally spaced, digital data should not be smaller than 25 cps. This calls for a sampling rate of at least 50 points per second.

5. Numerical, low-pass filtering can be used to filter out high-frequency errors introduced by hand digitization of the analog record. The low-pass filtered accelerogram can then be

differentiated for instrument correction purposes.

6. The recommended accelerometer instrument correction procedure consists of the numerical differentiation of the recorded transducer relative response function and use of the differential equation for the viscously damped single-degree-of-freedom linear oscillator.

# ACKNOWLEDGEMENTS

M. D. Trifunac
Lamont-Doherty Geological Observatory
of Columbia University and the
Earthquake Engineering Research
Laboratory of the California Institute
of Technology

F. E. Udwadia and A. G. Brady
Earthquake Engineering
Research Laboratory of the
California Institue of Technology

# REFERENCES

Hudson, D.E., A.G.Brady and M.D.Trifunac (1969). Strong-Motion Earthquake Accelerograms, Digitized and Plotted Data, Vol. I, Earthquake Engineering Research Laboratory, EERL 69-20, California Institute of Technology, Pasadena.

Jenschke, V.A. and J.Penzien (1964). Ground Motion Accelerogram Analysis Including Dynamical Instrumental Correction, Bull. Seism. Soc. Amer. 54 , 2087-2098.

McLennan, G.A. (1969). An Exact Correction for Accelerometer Error in Dynamic Seismic Analysis, Bull. Seism. Soc. Amer. 59 , 705-715.

Trifunac, M.D. and D.E.Hudson (1970). Laboratory Evaluations and Instrument Corrections of Strong-Motion Accelerographs, Earthquake Engineering Research Laboratory, EERL 70-04, California Institute of Technology, Pasadena.

Trifunac, M.D. (1970). Low Frequency Digitization Errors and a New Method for Zero Baseline Correction of Strong-Motion Accelerograms, Earthquake Engineering Research Laboratory, EERL 70-07, California Institute of Technology, Pasadena.